All possible first signals of gauge leptoquark in quark-lepton unification and beyond

Hedvika Gedeonová* and Matěj Hudec†
Institute of Particle and Nuclear Physics, Charles University, Prague, Czech Republic

(Received 19 October 2022; accepted 26 March 2023; published 19 May 2023)

We study possible current and future low-energy signals of the gauge leptoquark in quark-lepton $SU(4)$ unification *à la* Pati-Salam. Taking fully into account the freedom in the generation mixing between quarks and leptons, we compile a catalog of observables which currently form a border of the excluded part of the parameter space—hot candidates for first signals of new physics. We also determine the sensitivity needed in order to inspect a currently allowed part of the parameter space for several other measurements which are not included in this catalog. We improve older similar works on this topic by taking into account more (and more recent) experimental measurements and by scanning the parameter space more densely. Furthermore, we study in a similar manner the $SU(4)$ models with a small number of generations of extra leptons. We also discuss the minimal number of leptons needed in order to alleviate the contemporary discrepancies in the neutral-current B-meson decays.

DOI: 10.1103/PhysRevD.107.095029

I. INTRODUCTION

The main goal of this phenomenological study is to list all possible smoking gun signals of the Pati-Salam leptoquark.

A. Quark-lepton unification and gauge leptoquark

Quark-lepton unification (QLU) *à la* Pati and Salam [1,2] is an old idea motivated by the equal number of lepton and quark families and their similar electroweak behavior. Technically, QLU is based on extending the QCD gauge factor $SU(3)_C$ to $SU(4)_C$ and accommodating the quarks and leptons in common four-dimensional representations,

$$\begin{pmatrix} q_L \\ \ell_L \end{pmatrix}, \qquad \begin{pmatrix} u_R \\ \nu_R \end{pmatrix}, \qquad \begin{pmatrix} d_R \\ e_R \end{pmatrix}. \tag{1}$$

The most characteristic prediction of QLU is the existence of a gauge leptoquark (LQ) U_1 transforming as $(3, 1, +2/3)$ with respect to the Standard Model (SM) gauge group $G_{\rm SM} = SU(3)_C \times SU(2)_L \times U(1)_Y$. The LQ has the following interactions with the fermions from Eq. (1):

$$\mathcal{L}_{\rm int} = \frac{g_4}{\sqrt{2}} (\overline{\hat{q}_{L}}_i \gamma_\mu V_L \hat{\ell}_L{}^i + \overline{\hat{d}}_R \gamma_\mu V_R \hat{e}_R + \overline{\hat{u}}_R \gamma_\mu V'_R \hat{\nu}_R) U_1{}^\mu + \text{H.c.} \tag{2}$$

Here $i \in \{1, 2\}$ is an $SU(2)_L$ index; $\hat{d}_R, \hat{u}_R, \hat{e}_R, \hat{\nu}_R$ denote the family triplets of the same-charge fermions in the mass basis, e.g. $\overline{\hat{d}_R} = (\overline{d_R}, \overline{s_R}, \overline{b_R})$, and similarly $\hat{q}_L$ and $\hat{\ell}_L$ are in the mass basis of their $T^3_L = -1/2$ components. The 3×3 flavor matrices V_L, V_R, V'_R and the LQ mass m_{U_1} are free parameters of the theory. QLU fixes the g_4 coupling at the scale of $SU(4)_C$ breaking and restricts V_L, V_R, V'_R to unitary patterns, i.e.,

$$g_4(m_{U_1}) = g_3(m_{U_1}), \tag{3a}$$

$$V_L, V_R, V'_R \in U(3). \tag{3b}$$

For the derivation of these relations, see e.g., [2–5].

The interactions of U_1 conserve baryon and lepton numbers but always introduce lepton flavor violation (LFV) and lepton flavor universality violation (LFUV)—see Appendix A. Hence, the gauge leptoquark is not restricted by proton stability nor by searches for neutrinoless double-beta decay, while extraordinarily high-mass limits stem from flavor phenomenology: assuming $V_L = V_R = \mathbb{1}$, the experimental bound $\text{BR}(K^0_L \to e^\pm \mu^\mp) < 4.7 \times 10^{-12}$ [6] implies $m_{U_1} \gtrsim 2000$ TeV. However, the gauge leptoquark has different phenomenology with different forms of $V_{L,R}$.

*gedeonova@ipnp.mff.cuni.cz
†Corresponding author.
hudec@ipnp.mff.cuni.cz

B. Literature overview

Studies of the U_1 leptoquark have gained popularity in recent years as it has been identified as an excellent candidate to account for the neutral-current as well as charged-current B-meson anomalies (e.g., [7,8]). The benchmark setup for accommodation of the B anomalies as identified in Ref. [8] can be written as

$$\frac{g_4 V_L}{m_{U_1}} = \frac{1}{2\text{ TeV}} \begin{pmatrix} 0 & 0 & 0 \\ 0 & -0.05\xi & 0.6 \\ 0 & 0.05/\xi & 0.7 \end{pmatrix},$$
$$\frac{g_4 V_R}{m_{U_1}} = \begin{pmatrix} 0 & 0 & 0 \\ 0 & 0 & 0 \\ 0 & 0 & 0 \end{pmatrix}, \tag{4}$$

where ξ is a positive $O(1)$ number. Clearly, such flavor and chirality pattern is incompatible with the conditions in Eqs. (3). For this reason, most of the current studies employ chiral vector-LQ models, based on more complicated gauge groups or on complete abandonment of the gauge nature of the U_1 field.

Despite its inability to account for the discrepancies in the B-meson decays, the gauge leptoquark in the QLU framework is worth a detailed and dedicated study as it is a common feature of many specific models. Several top-down studies have already been published in the last decades.

In 1994, Valencia and Willenbrock [9] considered the cases where $V_L = V_R$ are permutation matrices, i.e., where each lepton is coupled to a single quark, and studied various two-body meson and tau decays. They found that apart from $K_L^0 \to e\mu$, the gauge LQ mass was for some mixing patterns limited from below to 250 TeV by $\mathrm{R}_{e/\mu}(\pi^+ \to l^+\nu)$ or $\mathrm{R}_{e/\mu}(K^+ \to l^+\nu)$, or by $\mathrm{BR}(B^+ \to e^+\nu)$ to $m_{U_1} > 13$ TeV. At around the same time, Kuznetsov and Mikheev [10] considered various (semi)leptonic K and π decays and the $\mu \to e$ conversion on nuclei, and cast inequalities employing m_{U_1} and elements of quark-lepton mixing matrices, virtually taking the full freedom in the quark-lepton mixing into account, but still tacitly assuming $V_L = V_R$. Apart from $\mathrm{BR}(K_L^0 \to e\mu)$ and $\mathrm{R}_{e/\mu}(K^+ \to l^+\nu)$, important bounds have been found to stem also from BR's of $K_L^0 \to l^+l^-$, $K \to \pi\mu e$ and from coherent $\mu \to e$ conversion on titanium nuclei. Needless to say, both analyses [9,10] are outdated nowadays due to new experimental data.

Concerning more recent works, Ref. [11] considered $K_L^0 \to e\mu$ and $B^0 \to e\tau$ for general forms of $V_{L,R}$ but did not confront the obtained limits with other measurements. In Ref. [12], which is the 2012 update of [10], also the B factory results on B and τ decays have been included and the general case $V_L \neq V_R$ has been considered. A specific form of V_L and V_R has been found for which the stated LQ mass limit was as low as 38 TeV. However, as pointed out in Ref. [4], this finding is invalid because the authors forgot to include the predictions for the $\mu^- e^+$ final state when studying $\mathrm{BR}(B^0 \to \mu^\pm e^\mp)$ and $\mathrm{BR}(B_s \to \mu^\pm e^\mp)$.

Finally, Smirnov [4] considered all kinematically allowed leptonic decays $P^0 \to l^+ l'^-$ for $P^0 = K_L^0, B^0, B_s$ and took fully into account the freedom in the fermion mixing by performing a scan. The global lower limit stemming from these processes was found to be

$$m_{U_1} > 86\text{ TeV}, \tag{5}$$

and the corresponding forms of V_L and V_R were given. We have verified the computations by completely recalculating Ref. [4].

C. Outline of our work

The main goal of this work is to identify all observables which currently determine the gauge LQ mass limit for some form of $V_{L,R} = (V_L, V_R)$. These observables are excellent candidates for future new physics (NP) signals since even a small improvement in the precision of their measurement shall explore a yet unexcluded part of the parameter space of the model. Hence, we call them possible first future signals of the gauge LQ.

Clearly, this is a more ambitious aim than just finding the global LQ mass limit which is the main result of Ref. [4].

In the analysis, we focus especially on the following:

(i) We attempt to take into account all relevant observables in which the signal of the gauge LQ in the foreseeable future might be potentially found. To this end, we employ the PYTHON package FLAVIO [13] which is capable of calculating predictions for hundreds of observables.

(ii) More recent measurements are included.

(iii) No *ad hoc* assumptions are made on the form of $V_{L,R}$. Keeping in mind that there is no physically meaningful measure on the parametric space, the setups which might be labeled as fine-tuned scenarios or small parts of the parameter space are not dismissed.

Section II describes the model in more detail. In Sec. III, the technicalities of the calculations are presented. In Sec. IV, we present the results and discuss the potential of various relevant forthcoming experiments. Then in Sec. V, we analyze in a similar manner the $SU(4)_C$ models extended by several generations of left- and/or right-handed leptons. We briefly conclude afterwards. In the three appendixes we provide some additional details concerning the lepton flavor group in LQ models, the physics of the Z' boson, and the optimization of the scanning procedure, respectively.

II. MODEL DETAILS

The $SU(4)_C$ gauge symmetry can be realized in a minimal way within the

$$G_{421} = SU(4)_C \times SU(2)_L \times U(1)_R \tag{6}$$

gauge group [3,5]. This symmetry might be an intermediate stage of a left-right theory based on the Pati-Salam group $G_{422} = SU(4)_C \times SU(2)_L \times SU(2)_R$ [1,2]. The spontaneous symmetry breaking (SSB) of G_{421} proceeds in two steps as

$$G_{421} \to G_{\mathrm{SM}} \to SU(3)_C \times U(1)_Q. \tag{7}$$

The generators $T_C^1, \ldots, T_C^8$ of the unbroken part of the $SU(4)_C$ symmetry form $SU(3)_C$, while the weak hypercharge is given by $Y = \sqrt{2/3} T_C^{15} + R$. During the first step of symmetry breaking, massive gauge leptoquark U_1 and massive Z' arise; the W and Z bosons acquire mass during the second step in a SM-like manner. For further details we refer to [3,5] or to Appendix B.

The fermion sector consists of three generations of the fields in Eq. (1). Independent quark and charged-lepton masses can be achieved by using both 1- and 15-dimensional scalar rep. of $SU(4)_C$ [2,3,5]. Concerning the neutrinos, in principle one can assume that they are of Dirac nature [3,14–17]. In such a case, the tiny neutrino masses are obtained as a difference of two parameters of the order of the top-quark mass. To avoid such a fine-tuning, one might call for some form of a seesaw mechanism. The traditional type-I seesaw (studied recently in Ref. [18] in this context) would require that the $SU(4)_C$ breaking scale is so high that the gauge LQ would have no measurable low-energy phenomenology; hence, this case is not of interest for us. Nevertheless, unification of quarks and leptons is possible even at a low scale when employing the inverse seesaw [5,18] instead. This model has been recently studied in context of the B anomalies addressed by the *scalar* leptoquarks by Faber *et al.* [19,20] and also by Fileviez Pérez *et al.* [21,22] with mutually conflicting conclusions.

In accordance with the inverse-seesaw model, we assume heavy ν_R in this study. Nevertheless, as we shortly discuss in Sec. IV, the results would be essentially identical also in the (fine-tuned) Dirac-neutrino case.

The interplay among the flavor matrices V_L, V_R, V'_R introduced in Eq. (2) and the weak interaction matrices V_{PMNS} and V_{CKM} is illustrated in Fig. 1. Adopting the standard (single-phase) parametrization of V_{CKM} and V_{PMNS}, no complex phases can be removed from V_L or V_R. By expanding the $SU(2)_L$ structure in Eq. (2), the interactions of the SM fermions with the gauge LQ can be rewritten as

$$\mathcal{L}_{U_1} = \frac{g_4}{\sqrt{2}} (\bar{\hat{d}} \gamma^\mu [\mathbb{P}_L V_L + \mathbb{P}_R V_R] \hat{e} + \overline{\hat{u}_L} \gamma^\mu V_{\mathrm{CKM}} V_L \tilde{\nu}_L) U_{1\mu} + \mathrm{H.c}, \tag{8}$$

where $\tilde{\nu}$ is a neutrino flavor triplet in the weak interaction basis and $\mathbb{P}_{L,R} = (1 \mp \gamma_5)/2$ are chirality projectors. As the

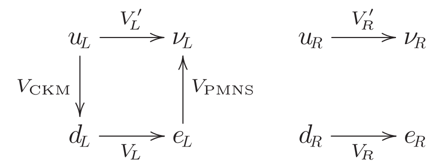

FIG. 1. Scheme of fermion mixing in the quark-lepton symmetry models based on the G_{421} gauge group. Here $V'_L = V_{\mathrm{CKM}} V_L V_{\mathrm{PMNS}}$.

particular form of the V'_R matrix is inconsequential for all the considered low-energy processes, the relevant dimensions of the parameter space are given solely by 2×9 angles or phases of $V_{L,R}$ and by m_{U_1}.

We do not take into account any other BSM field in the model. Especially, the scalar sector is neglected. Note that the free parameters of the full renormalizable model [5] (or [3]) indeed allow for the regime in which the gauge LQ signals dominate over those of the scalars. Notice also that the interactions of Z' are flavor-diagonal and hence, its effects in flavor physics are suppressed. If there is no intermediate stage in the $G_{421} \to G_{\mathrm{SM}}$ symmetry breaking, $m_{Z'}$ is of the same order as m_{U_1}; in such a case, Z' can be also safely neglected. For more details, see Appendix B.

III. METHODS

In what follows, by parameter space we mean the 18-dimensional set of forms of $V_{L,R}$. A parameter point is an element of this set, parametrized by angles and phases $\lambda_{L,ij}$ and $\lambda_{R,ij}$ as described in Appendix C.

We have employed two different approaches to investigate a chosen parameter point. The simplified approach, adopted from Ref. [4] and detailed in Sec. III A, served as a primary stage providing basic but yet coherent insight into the parameter space. Within the concept, the identification of interesting parts of the parameter space was quite straightforward since it makes use of simple analytical formulas for observable predictions. The more robust approach, described in Sec. III B, is more comprehensive, but also much less intuitive since it is based on numerical packages which we have used mostly as a black-box tool.

The former approach served also as an important crosscheck which enabled us to find and correct an error in the FLAVIO package.[1] Hence, even tough the presented results are based solely on the latter, we still find it worthy to present also the first approach below.

In Sec. III C, we describe how the analyzed parameter points have been chosen.

A. Simplified approach

This approach directly follows Ref. [4]. There are several aspects about this procedure worth mentioning:

[1]There was a bug in the expression for the $K^0_{L,S} \to e^\pm \mu^\mp$ amplitudes.

(1) The effects of the U_1 leptoquark are taken into account at the tree level.
(2) Four-loop QCD running of the induced effective operators is taken into account [23]. For simplicity, the effective operators are defined at the 100 TeV scale, regardless of the considered LQ mass.
(3) SM contributions to the considered processes are completely neglected in the calculation. To highlight this approximation, the corresponding predictions for branching ratios are labelled by BR_V. The measured BR's of the decays which have been already observed (i.e., $K_L^0 \to ee$, $K_L^0 \to \mu\mu$, $B_s^0 \to \mu\mu$) are taken as limits on BR_V. Such a rough approximation is meaningful due to large relative theoretical uncertainties for the SM amplitudes.
(4) Reference [4] has taken into account the branching ratios of $P \to l^\pm l'^\mp$ decays where $P = K_L^0, B^0, B_s^0$ and ll' corresponds to various kinematically allowed combinations of leptons and antileptons. In our work, also the leptonic decays of K_S^0 are considered. The limits on $B_{d,s}^0 \to e^\pm \mu^\mp$ are updated [24].
(5) No processes with neutrinos are analyzed; the study holds for both situations with light or heavy right-handed neutrinos.
(6) The masses of electrons and muons in the final state are neglected, as well as the indirect CP violation in the neutral kaon mass eigenstates.
(7) For given $V_{L,R}$, the LQ mass limit is determined as the maximum of individual limits obtained from the considered observables. The decay responsible for the strongest limit is considered to be the candidate for the future first signal of the LQ for the investigated form of $V_{L,R}$.

The branching ratio for a decay with light leptons only is calculated by the following formula:

$$\mathrm{BR}_V(P \to l^+ l'^-) = \frac{m_P \pi \alpha_s^2 f_P^2 \bar{m}_P^2 (R_P^V)^2}{2 m_{U_1}^4 \Gamma_P^{\mathrm{tot}}} \beta_{P,ll'}^2, \qquad (9)$$

where the form factors are $f_K = 155.72$ MeV, $f_{B^0} = 190.9$ MeV, $f_{B_s^0} = 227.2$ MeV, and $\bar{m}_P = m_P^2/(m_{\bar{q}} + m_q)$ with $\bar{q}$ and q standing for the index of the valence antiquark and quark of P, respectively. The gluonic corrections to the pseudoscalar quark currents amount to $R_K^V = 3.47$ and $R_B^V = 2.1$ [23]. The lepton-flavor-dependent factor is a sum over two different helicity combinations

$$\beta_{P,ll'}^2 = \frac{|a_{LR}(P,l,l')|^2 + |a_{RL}(P,l,l')|^2}{2}, \qquad (10)$$

where for weak eigenstates

$$a_{LR}(P,l,l') = (V_L)_{\bar{q}l} (V_R)^*_{ql'}, \qquad (11a)$$

$$a_{RL}(P,l,l') = (V_R)_{\bar{q}l} (V_L)^*_{ql'}, \qquad (11b)$$

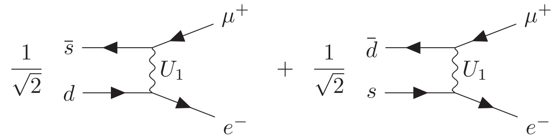

FIG. 2. A tree-level LFV decay of K_L^0.

while for the CP eigenstates,

$$a(K_{L,S}^0, l, l') = \frac{a(K^0,l,l') \pm a(\bar{K}^0,l,l')}{\sqrt{2}}. \qquad (12)$$

Here + and − relate to K_L^0 and K_S^0, respectively, and a stands for either a_{LR} or a_{RL}. See Fig. 2 for an illustration.

For processes with a single τ lepton in the final state, the expression for BR_V in Eq. (9) must be multiplied by a phase space factor $(1 - m_\tau^2/m_P^2)^2$. Along with that, the replacement $(V_{L,R})_{r\tau} \to [(V_{L,R})_{r\tau} - (V_{R,L})_{r\tau} m_\tau/(2\bar{m}_P R_P^V)]$ for $r = q, \bar{q}$ is applied in Eq. (11). For $\tau^+\tau^-$ in the final state see Ref. [4].

B. More robust approach

In parallel with the previous approach, we have also performed a similar analysis using the family of general-purpose open-source tools wilson [25,26], FLAVIO [13,27], and SMELLI [28,29]. We present the features of this approach as a list which can be compared with that in the previous section.

(1) The LQ interactions are matched onto the Standard Model effective field theory (SMEFT) at the tree level (similarly to the previous approach), yielding nonzero wilson coefficients

$$C_{ed\_\bar{l}l\bar{q}q} = -1 \frac{g_4^2}{2m_{U_1}^2} (V_R)^*_{q\bar{l}} (V_R)_{\bar{q}l}, \qquad (13a)$$

$$C_{\ell edq\_\bar{l}l\bar{q}q} = +2 \frac{g_4^2}{2m_{U_1}^2} (V_R)^*_{q\bar{l}} (V_L)_{\bar{q}l}, \qquad (13b)$$

$$C^{(1)}_{\ell q\_\bar{l}l\bar{q}q} = C^{(3)}_{\ell q\_\bar{l}l\bar{q}q} = -\frac{1}{2} \frac{g_4^2}{2m_{U_1}^2} (V_L)^*_{q\bar{l}} (V_L)_{\bar{q}l}, \qquad (13c)$$

which multiply the following effective operators (with flavor indices suppressed),

$$\mathcal{O}_{ed} = (\overline{e_R}\gamma_\mu e_R)(\overline{d_R}\gamma^\mu d_R), \qquad (14a)$$

$$\mathcal{O}_{\ell edq} = (\overline{\ell_L} e_R)(\overline{d_R} q_L), \qquad (14b)$$

$$\mathcal{O}^{(1)}_{\ell q} + \mathcal{O}^{(3)}_{\ell q} = (\overline{\ell_L}\gamma_\mu \ell_L)(\overline{q_L}\gamma^\mu q_L) + (\overline{\ell_L}\gamma_\mu \sigma^I \ell_L)(\overline{q_L}\gamma^\mu \sigma^I q_L). \qquad (14c)$$

We have implemented a PYTHON function taking $V_{L,R}$ and m_{U_1} as input arguments and returning a dictionary of SMEFT wilson coefficients in the format compatible with the WCxf standard [30,31], which is used by the packages mentioned above.

(2) The renormalization group (RG) running of the SMEFT effective operators from the scale $\mu = m_{U_1}$ to the electroweak scale, the tree level matching onto the weak effective theory (WET) and further evolution to the meson-mass energy scales is handled automatically by the wilson package. The full numerical solution to the one-loop SMEFT RG equations (the `'integrate'` option) is performed since we have exemplified that the `'leadinglog'` approximation leads to $O(1)$ relative differences in certain predictions. Analytical solution to the one-loop QCD and QED running equations is applied under the electroweak scale in wilson. For more details see Ref. [25] and references therein.

(3) The SM contributions to the amplitudes of the calculated processes are automatically taken into account by FLAVIO. As a result of this (and of the RG running), the predictions do not scale uniformly as $m_{U_1}^{-4}$, which was a simplifying feature of the previous approach [see Eq. (9)].

(4) The global likelihood tool SMELLI is employed. This package uses FLAVIO for predictions and confronts them with the measurements, including correlations. By default, version 2.2.0 of SMELLI takes into account hundreds of observables, most of which are, however, irrelevant for our scenarios. On the other hand, the very interesting processes $\mathrm{BR}(B^0_{d,s} \to e^+e^-)$ as well as $\mu \to e$ conversion on nuclei were not included. To this end, we have modified the SMELLI package to calculate also these observables.

The complete list of considered observables can be found in [32] or inferred from [33].

(5) No light right-handed neutrinos are assumed.

(6) Light lepton masses are taken into account in FLAVIO for all observables, but indirect CP violation in neutral kaons remains neglected in the $K^0_{L,S} \to ll'$ decays.

(7) For V_L and V_R fixed, we find m_{U_1} for which the global log-likelihood calculated by SMELLI worsens by four units with respect to the SM. That value defines the lower LQ mass limit for this particular case. Then, the corresponding candidate for the future first signal of NP is the observable for which the individual pull between theory and experiment worsened the most compared to the SM case; the pulls have been obtained via the `obstable` method provided by the SMELLI package [28].

We have also tried different (more complicated) criteria, supposed to underpin scenarios in which the likelihood actually improves, but we ended up with qualitatively identical results.

C. Analyzing the parameter space

The final analysis has been performed within the more robust approach where analyzing a single parameter point typically takes over a minute on a usual computer. Apparently, an 18-dimensional parameter space cannot be rigorously explored just with a blind numerical scan. To this end, we have addressed the issue in two mutually complementary ways:

(i) A series of random numerical scans has been performed, using a naïve measure $\Pi_{ij} \mathrm{d}\lambda_{L,ij} \mathrm{d}\lambda_{R,ij}$, where i, j run only over the unfixed λ's. The gradual fixing of λ's proceeded along the following lines (the details can be found in Appendix C).

In the first stage, 10^3 parameter points have been obtained with none of the λ's fixed. In majority of cases, the limiting processes were $\mathrm{BR}(K^0_L \to e\mu)$, $\mathrm{BR}(K^0_L \to ee)$ and $\mathrm{CR}(\mu \to e, \mathrm{Au})$, i.e., the coherent conversion rate of $\mu \to e$ on nuclei.

Following Ref. [4] in the second stage, about 2×10^3 parameter points have been obtained on the parameter subspace defined by $\mathrm{BR}_V(K^0_L \to ll') = 0$, achieved by Eqs. (C10) and (C11). This is motivated by exploring the "steep valleys" on Fig. 3. Now $\mathrm{CR}(\mu \to e, \mathrm{Au})$ dominated almost all cases.

In the third stage, more than 10^4 parameter points have been obtained by random scanning on the parameter subspace restricted both by $\mathrm{BR}_V(K^0_L \to ll') = 0$ and $\mathrm{CR}(\mu \to e, \mathrm{Au}) \approx 0$, i.e., by Eqs. (C10), (C11), and (C13).

(ii) We have compiled a list of relevant observables discussed in the recent review in Ref. [34] and investigated if they might become the future first signal. For each of these observables, we have found either a parameter point for which this observable is the first future signal indeed, or an argument that such a point should not exist. A thorough effort has

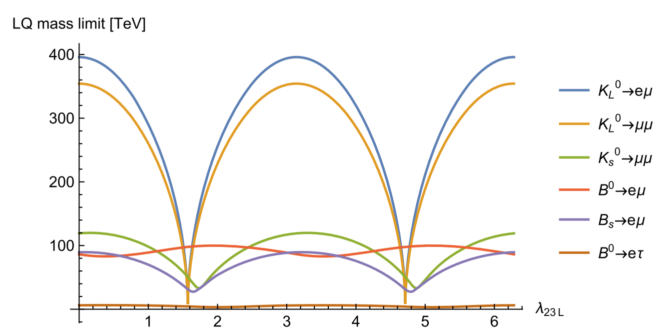

FIG. 3. Illustration of lower limits on the gauge LQ mass stemming from several observables, calculated along a one-dimensional cut of the parameter space. The parameter λ_{23L} is defined by the composite parametrization as introduced in Appendix C. On this slice of the parameter space, the bounds are given by $\mathrm{BR}(K^0_L \to e^\pm\mu^\mp)$ and $\mathrm{BR}(B^0 \to e^\pm\mu^\mp)$. The mass limits are obtained using the approach described in Sec. III A.

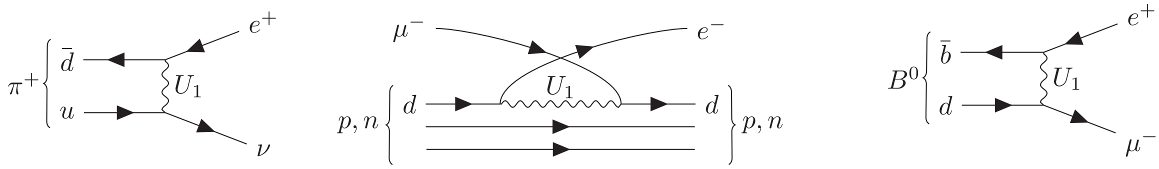

FIG. 4. Examples of Feynman graphs underpinning the possible first signals of the U_1 gauge leptoquark.

been made to include various special parts of the parameter space in the considerations.

Combining those two methods enables us to claim with a higher level of confidence that the catalog in Table I is complete.

IV. RESULTS

Tables I and II present the catalog of observables which currently give the most stringent constraint on m_{U_1} for some configuration of $V_{L,R}$ (see also Fig. 4). These observables correspond to the future first signals as defined above. To fully appreciate the result, notice that even a very small improvement in precision of any experimental limit listed in Table I will probe a so-far allowed part of the parameter space of the model, and could potentially detect a NP signal—the only exception is the observed decay $K_L^0 \to \mu\mu$ for which the theoretical uncertainties within the SM dominate.

Conversely, under a very idealized assumption that the experimental sensitivity will grow uniformly for all the observables considered, no other observable could become the first observed signal of the gauge LQ. More realistically, the measurement precision of any other observable needs to be improved by a larger step in order to put a new constraint on the model parameters or to have a theoretical chance of observing a signal of the gauge LQ. How large these steps must be is shown for several important examples in Table III.

A. Global mass limit: Comparison with Ref. [4]

As noted earlier, the simplified approach of Ref. [4] described in Sec. III A leads to the global lower leptoquark mass limit of 86 TeV. The corresponding $V_{L,R}$ is shown in the last line of Table II. However, when taking into account more observables in the more robust approach, $m_{U_1} = 86$ TeV for this parameter point turns out to be in conflict with the bound on $\mathrm{CR}(\mu \to e, \mathrm{Au})$ by three orders of magnitude.

Nevertheless, we have found a form of $V_{L,R}$ which allows essentially the same mass (90 TeV, see Table II) even when all the constraints included in SMELLI are considered.

B. Possible first signals

Concerning searches for LFV, Table I contains limits on $K_L^0, B_{d,s}^0 \to e\mu$ and on the $\mu \to e$ coherent conversion on nuclei; further searches for these processes are therefore of great interest. The remaining observables in Table I are all related to the leptonic decays of pseudoscalar mesons which are chirality suppressed in the SM and can be understood as tests of LFUV in the SM.

Firstly, significant deviations could arise in the ratios of charged-current decays $R_{e/\mu}(P^+ \to l\nu)$ with $P = \pi,\ K$ when the LQ couples mostly to the electrons. Although the decay widths involved cannot be measured with the precision similar to the rare decays above, the deviations

TABLE I. Complete list of observables which currently constrain the gauge LQ mass for some form of the $V_{L,R}$ matrices. The experimental limits are given at 90% CL. The SM predictions have been calculated in FLAVIO unless cited.

Observable	Experiment	SM prediction
$\mathrm{BR}(K_L^0 \to e^\pm \mu^\mp)$	$<4.7 \times 10^{-12}$ [6]	0
$\mathrm{BR}(K_L^0 \to e^+ e^-)$	$8.7^{+5.7}_{-4.1} \times 10^{-12}$ [35]	$(9.0 \pm 0.5) \times 10^{-12}$ [36,37]
$\mathrm{BR}(K_L^0 \to \mu^+ \mu^-)$	$(6.84 \pm 0.11) \times 10^{-9}$ [38]	$(7.4 \pm 1.3) \times 10^{-9}$
$\mathrm{BR}(K_S^0 \to \mu^+ \mu^-)$	$<2.1 \times 10^{-10}$ [39]	$(5.2 \pm 1.5) \times 10^{-12}$ [40]
$\mathrm{BR}(B^0 \to e^\pm \mu^\mp)$	$<1.0 \times 10^{-9}$ [41]	0
$\mathrm{BR}(B_s \to e^\pm \mu^\mp)$	$<5.4 \times 10^{-9}$ [41]	0
$\mathrm{BR}(B^0 \to \mu^+ \mu^-)$	$1.1^{+1.4}_{-1.3} \times 10^{-10}$ [38]	$(1.1 \pm 0.1) \times 10^{-10}$
$\mathrm{BR}(B_s \to \mu^+ \mu^-)$	$(3.0 \pm 0.4) \times 10^{-9}$ [38]	$(3.7 \pm 0.2) \times 10^{-9}$
$\mathrm{R}_{e/\mu}(\pi^+ \to l^+ \nu)$	$1.2327(23) \times 10^{-4}$ [38]	$1.2352(1) \times 10^{-4}$ [42]
$\mathrm{R}_{e/\mu}(K^+ \to l^+ \nu)$	$2.488(9) \times 10^{-5}$ [38]	$2.476(2) \times 10^{-5}$
$\mathrm{CR}(\mu \to e, \mathrm{Au})$	$<7 \times 10^{-13}$ [43]	0

TABLE II. Examples of quark-lepton mixing matrices and the corresponding dominant signals of the gauge leptoquark.

Observable	V_L	V_R	Limit on m_{U_1}/TeV
$\mathrm{BR}(K_L^0 \to e\mu)$	$\begin{pmatrix} 1 & 0 & 0 \\ 0 & 1 & 0 \\ 0 & 0 & 1 \end{pmatrix}$	$\begin{pmatrix} 1 & 0 & 0 \\ 0 & 1 & 0 \\ 0 & 0 & 1 \end{pmatrix}$	2074
$\mathrm{BR}(K_L^0 \to ee)$	$\begin{pmatrix} \frac{1}{\sqrt{2}} & 0 & \frac{1}{\sqrt{2}} \\ \frac{1}{\sqrt{2}} & 0 & -\frac{1}{\sqrt{2}} \\ 0 & 1 & 0 \end{pmatrix}$	$\begin{pmatrix} \frac{1}{\sqrt{2}} & 0 & \frac{1}{\sqrt{2}} \\ \frac{1}{\sqrt{2}} & 0 & -\frac{1}{\sqrt{2}} \\ 0 & 1 & 0 \end{pmatrix}$	1335
$\mathrm{BR}(K_L^0 \to \mu\mu)$	$\begin{pmatrix} 0 & \frac{1}{\sqrt{2}} & \frac{1}{\sqrt{2}} \\ 0 & \frac{1}{\sqrt{2}} & -\frac{1}{\sqrt{2}} \\ 1 & 0 & 0 \end{pmatrix}$	$\begin{pmatrix} 0 & \frac{1}{\sqrt{2}} & \frac{1}{\sqrt{2}} \\ 0 & \frac{1}{\sqrt{2}} & -\frac{1}{\sqrt{2}} \\ 1 & 0 & 0 \end{pmatrix}$	319
$\mathrm{BR}(K_S^0 \to \mu\mu)$	$\begin{pmatrix} 0 & \frac{1}{\sqrt{2}} & \frac{1}{\sqrt{2}} \\ 0 & \frac{1}{\sqrt{2}} & -\frac{1}{\sqrt{2}} \\ 1 & 0 & 0 \end{pmatrix}$	$\begin{pmatrix} 0 & \frac{1}{\sqrt{2}} & \frac{1}{\sqrt{2}} \\ 0 & -\frac{1}{\sqrt{2}} & -\frac{1}{\sqrt{2}} \\ 1 & 0 & 0 \end{pmatrix}$	153
$\mathrm{BR}(B^0 \to \mu\mu)$	$\begin{pmatrix} 0 & -\frac{1}{\sqrt{21}} & -\sqrt{\frac{20}{21}} \\ 0 & -\sqrt{\frac{20}{21}} & \frac{1}{\sqrt{21}} \\ -1 & 0 & 0 \end{pmatrix}$	$\begin{pmatrix} -\frac{1}{\sqrt{21}} & 0 & -\sqrt{\frac{20}{21}} \\ \sqrt{\frac{20}{21}} & 0 & -\frac{1}{\sqrt{21}} \\ 0 & -1 & 0 \end{pmatrix}$	102
$\mathrm{BR}(B_s \to \mu\mu)$	$\begin{pmatrix} 0. & 0. & i \\ -0.26-0.34i & 0.78-0.45i & 0. \\ -0.74-0.52i & -0.29+0.32i & 0. \end{pmatrix}$	$\begin{pmatrix} 0. & 0. & 1 \\ 0.20-0.29i & 0.83-0.43i & 0. \\ -0.14-0.92i & -0.12+0.34i & 0. \end{pmatrix}$	290
$\mathrm{BR}(B^0 \to e\mu)$	$\begin{pmatrix} 0 & -1 & 0 \\ 0 & 0 & 1 \\ -1 & 0 & 0 \end{pmatrix}$	$\begin{pmatrix} 0 & -1 & 0 \\ 0 & 0 & 1 \\ -1 & 0 & 0 \end{pmatrix}$	123
$\mathrm{BR}(B_s \to e\mu)$	$\begin{pmatrix} 0 & -0.04-0.06i & -0.09-0.99i \\ 0 & 0.20-0.98i & -0.05+0.06i \\ 1 & 0 & 0 \end{pmatrix}$	$\begin{pmatrix} 0 & -0.06+0.04i & -0.23-0.97i \\ 0 & 0.12-0.99i & -0.06-0.04i \\ 1 & 0 & 0 \end{pmatrix}$	90
$\mathrm{R}_{e/\mu}(K^+ \to l\nu)$	$\begin{pmatrix} 0 & 0 & 1 \\ 1 & 0 & 0 \\ 0 & 1 & 0 \end{pmatrix}$	$\begin{pmatrix} 0 & 0 & 1 \\ 1 & 0 & 0 \\ 0 & 1 & 0 \end{pmatrix}$	245
$\mathrm{R}_{e/\mu}(\pi^+ \to l\nu)$	$\begin{pmatrix} 1 & 0 & 0 \\ 0 & 0 & 1 \\ 0 & 1 & 0 \end{pmatrix}$	$\begin{pmatrix} 1 & 0 & 0 \\ 0 & 0 & 1 \\ 0 & 1 & 0 \end{pmatrix}$	270
$\mathrm{CR}(\mu \to e, \mathrm{Au})$	$\begin{pmatrix} 0.38 & 0 & 0.93 \\ -0.93i & 0 & 0.38i \\ 0 & i & 0 \end{pmatrix}$	$\begin{pmatrix} 0.26 & 0.27 & 0.93 \\ -0.64i & -0.67i & +0.38i \\ -0.72i & +0.69i & 0 \end{pmatrix}$	585

TABLE III. Examples of processes which are not listed in Table I. The third column shows predictions obtained during the numerical scanning following from the forms of V_L, V_R, and m_{U_1} which are fully compatible with all the current experimental limits. We also list the SM predictions for comparison.

Observable	Experimental limit	QLU model prediction	SM prediction
$\mathrm{BR}(K_S^0 \to e^+e^-)$	$<9 \times 10^{-9}$ [44]	$\leq 2 \times 10^{-9}$	2×10^{-14} [44]
$\mathrm{BR}(K_S^0 \to e^\pm\mu^\mp)$	N/A [38]	$\leq 3 \times 10^{-10}$	0
$\mathrm{BR}(B^0 \to e^+e^-)$	$<2.5 \times 10^{-9}$ [45]	$\leq 1.1 \times 10^{-10}$	3×10^{-15} [46]
$\mathrm{BR}(B_s \to e^+e^-)$	$<9.4 \times 10^{-9}$ [45]	$\leq 3 \times 10^{-9}$	9×10^{-14} [46]
$\mathrm{BR}(B^0 \to e^\pm\tau^\mp)$	$<2.8 \times 10^{-5}$ [47]	$\leq 6 \times 10^{-9}$	0
$\mathrm{BR}(B_s \to e^\pm\tau^\mp)$	N/A [38]	$\leq 2.5 \times 10^{-9}$	0
$\mathrm{BR}(B^0 \to \mu^\pm\tau^\mp)$	$<1.2 \times 10^{-5}$ [24]	$\leq 5 \times 10^{-9}$	0
$\mathrm{BR}(B_s \to \mu^\pm\tau^\mp)$	$<3.4 \times 10^{-5}$ [24]	$\leq 2.3 \times 10^{-9}$	0
$\mathrm{BR}(B^0 \to \tau^+\tau^-)$	$<1.6 \times 10^{-3}$ [48]	2×10^{-8}	2×10^{-8} [46]
$\mathrm{BR}(B_s \to \tau^+\tau^-)$	$<5.2 \times 10^{-3}$ [48]	8×10^{-7}	8×10^{-7} [46]

from the SM can be significant due to the interference among the NP and SM amplitudes. Subdominant contributions arise also from the other neutrino species as well as from the $l_L \nu_R$ final state if the right-handed neutrinos are light enough.

Secondly, limits on m_{U_1} stem also from the observed BRs of $K_L^0 \to ee, \mu\mu$ and $B_{d,s}^0 \to \mu\mu$. Concerning $K_L^0 \to \mu\mu$, the experimental precision is better than the theoretical error estimates in the SM stemming from long-distance contributions [49,50].

Finally, a very interesting limit on the U_1 mass for some patterns of quark-lepton mixing is set by the recent LHCb search for $K_S^0 \to \mu\mu$; the anticipated discovery of this decay after the upcoming LHC runs thus provides an exciting opportunity for the Pati-Salam-type leptoquark.

C. Other observables

In Table III, the $P^0 \to ll'$ decays that currently do not pose the most stringent bound on m_{U_1} are listed, together with the predictions based on the parameters fully compatible with all the current experimental searches. All generated parameter points have been included.

As τ leptons are generally experimentally hard to handle, all processes involving τ's belong to this category. In fact, 3–4 orders of magnitude improvements in limits on $B_{d,s}^0 \to l\tau$ would be necessary in order to compete with the other constraints, which is far below the prospected sensitivity of Belle II [51] and hardly achievable even at LHCb at the high-luminosity phase. Furthermore, as explained in Appendix C, due to the unitarity of $V_{L,R}$, the LQ amplitudes mediating of $B_{d,s}^0 \to \tau\tau$ are severely limited by the probes of $K_L^0 \to ll'$ and, thus, our predictions for the former essentially coincide with the SM. Hence, the expected sensitivity of Belle II at about 10^{-6} for $\mathrm{BR}(B^0 \to \tau\tau)$ [52] shall not be an interesting probe of the considered model.

On the other hand, the experimental sensitivities to K_S^0, B^0, and B_s decays to e^+e^- require less than one order of magnitude improvement in order to probe the currently unexplored parts of the parameter space. Note that $\mathrm{BR}_V(B_{d,s}^0 \to e^+e^-) = \mathrm{BR}_V(B_{d,s}^0 \to \mu^+\mu^-)$ is predicted for any parameter point for which $\mathrm{BR}_V(K_L^0 \to ll') = 0$ [4]; currently, the muonic channel is measured more accurately. However, when further searches for NP in the $P^0 \to \mu^+\mu^-$ decays become limited by the SM uncertainties, new searches for $B_{d,s}^0, K_S^0 \to ee$ will become essential.

No experimental limits on the decay $K_S^0 \to e\mu$ are available [38]. Comparing with the current limits on $K_S^0 \to ee$ [44] and $K_S^0 \to \mu\mu$ [39], we reckon the required experimental sensitivity around 10^{-10} for $K_S^0 \to e\mu$ might be reachable by KLOE II or LHCb.

Semileptonic decays like $B \to K\mu\mu$ or loop processes such as $\mu \to e\gamma$ might become the dominant signals of chiral leptoquaks but not of the gauge LQ in the considered model as it inevitably introduces sizable wilson coefficients $C_{\ell edq}$ which are experimentally more constrained (see, e.g., Ref. [53]).

V. EXTENDED $SU(4)_C$ MODELS

This part of our work is devoted to more complicated models featuring the vector leptoquark U_1. Although they could be considered as aesthetically less appealing, such models have been studied thoroughly in the recent years, mainly due to the attempts to accommodate the B-meson anomalies. Generally, several tricks to circumvent the theoretical requirement of unitarity of V_L and V_R have been suggested in the literature. They can be divided into three categories, according to the paradigm abandoned:

(1) Adding extra generations of fermions while maintaining the gauge symmetry group G_{421} or G_{422} [54–57].

(2) Assuming more complicated gauge structure. Especially, the models based on the $G_{4N21} = SU(4)_{C_L} \times SU(N)_{C_R} \times SU(2)_L \times U(1)_R$ gauge symmetry have become popular; here $N = 3$ or 4 and the QCD generators are given by $T_C^A = T_{C_L}^A + T_{C_R}^A$ for $A = 1, \ldots, 8$. In the basic setting of chiral quark-lepton symmetry [58,59], the left-handed fermions are charged by $SU(4)_{C_L}$ while the right-handed ones transform nontrivially under $SU(N)_{C_R}$. Hence, the U_1^μ field interacting with the left-handed quark-lepton currents is a chiral leptoquark—it has no or suppressed couplings to the right-handed currents, avoiding the scalar-type effective operators $\mathcal{O}_{\ell edq}$ which are responsible for all the most stringent limits in Table I.

In more general cases with $N = 3$, some quark and lepton fields are unified within the $SU(4)$ factor while others live in separate irreps of $SU(3)$ [60]. Usually, more than three generations of fermions are considered [61–65].

For even more exotic gauge groups see, e.g., [66,67].

(3) Assuming that the vector LQ is not a gauge field but a composite resonance formed by some more fundamental strongly interacting fields [68–70].

This work is focusing solely on the first option. Since the SM leptons do not entirely stem from the same $SU(4)_C$ representations as the quarks, we shall not use the term quark-lepton unification for these theories but rather call them extended $SU(4)_C$ models.

A. Specification of the models

Like in the previously considered $SU(4)_C \times SU(2)_L \times U(1)_R$ scenarios, see Eq. (1), the models contain three generations of each of the following chiral fermion $SU(4)_C$ quadruplets:

$$F_{L(4,2,0)} = \begin{pmatrix} q_L \\ {}^4\ell_L \end{pmatrix}, \tag{15a}$$

$$f^u_{R(4,1,+1/2)} = \begin{pmatrix} u_R \\ {}^4\nu_R \end{pmatrix}, \tag{15b}$$

$$f^d_{R(4,1,-1/2)} = \begin{pmatrix} d_R \\ {}^4e_R \end{pmatrix}. \tag{15c}$$

Notice that we have slightly updated the notation by adding an "isotopic index" to the leptons living inside the quadruplets. On top of that, k_L generations of $SU(2)_L$-doublet vectorlike fermions

$${}^1\ell_{L(1,2,+1/2)} + {}^1\ell_{R(1,2,+1/2)} \tag{16}$$

and k_R generations of weak-singlet vectorlike fermions

$${}^1e_{L(1,1,-1)} + {}^1e_{R(1,1,-1)}, \tag{17}$$

are assumed. Being $SU(4)_C$ singlets, these new fields are intact to interactions of the gauge LQ. After the $G_{421} \to G_{\rm SM}$ symmetry breaking, they can mix with the leptons from the quadruplets. We assume that the three lightest eigenstates correspond to e, μ, and τ, while the $k_L + k_R$ remaining ones are too heavy to be observed. As the weak hypercharges of the three known leptons are quite precisely measured, they must be composed solely from the fields ${}^1e_R, {}^4e_R, {}^1\ell_L$, and ${}^4\ell_L$. For all practical purposes, it is sufficient to assume the following mixing pattern in the charged-lepton sector:

$$\begin{pmatrix} \hat{e}_R \\ E_R \\ {}^1\ell_R^- \end{pmatrix} = \begin{pmatrix} \multicolumn{2}{c}{V^e_R} & 0_{3\times k_L} \\ & & 0_{k_R\times k_L} \\ 0_{k_L\times 3} & 0_{k_L\times k_R} & \mathbb{1}_{k_L\times k_L} \end{pmatrix} \begin{pmatrix} {}^4e_R \\ {}^1e_R \\ {}^1\ell_R^- \end{pmatrix}, \tag{18}$$

$$\begin{pmatrix} \hat{e}_L \\ E_L \\ {}^1e_L \end{pmatrix} = \begin{pmatrix} \multicolumn{2}{c}{V^e_L} & 0_{3\times k_R} \\ & & 0_{k_L\times k_R} \\ 0_{k_R\times 3} & 0_{k_R\times k_L} & \mathbb{1}_{k_R\times k_R} \end{pmatrix} \begin{pmatrix} {}^4\ell_L^- \\ {}^1\ell_L^- \\ {}^1e_L \end{pmatrix}, \tag{19}$$

where, generally, ℓ^- denotes the electrically charged component of an ℓ doublet (notice that ${}^1e_L \neq {}^1\ell_L^-$ and ${}^1e_R \neq {}^1\ell_R^-$), $\hat{e} = \hat{e}_L + \hat{e}_R$ is the triplet of light leptons while E_R and ${}^1\ell_R^-$ with their chiral counterparts E_L and ${}^1e_L$ form the heavy-mass eigenstates. The form of the mixing in the heavy-lepton sector is irrelevant for our considerations. The blocks V^e_L and V^e_R are arbitrary unitary matrices of dimension $3 + k_L$ and $3 + k_R$, respectively. Including the "nonstandard" fields ${}^1\ell_R$ and ${}^1e_L$ into the model ensures the ABJ anomaly cancellation and enables one to write down arbitrarily large Dirac mass terms for the vectorlike pairs.

The $Q = 0$ components of ${}^4\ell_L$ and ${}^1\ell_L$ naturally follow their charged $SU(2)_L$ partners during the mixing at the first stage of SSB: those belonging to E_L become equally heavy while the companions of $\hat{e}_L$ become the light neutrinos, eventually gaining mass after the electroweak symmetry breaking.

There are no extra quarks in the models and the transformation from gauge to mass eigenstates is given by 3×3 unitary matrices:

$$\hat{u}_L = V^u_L u_L, \qquad \hat{u}_R = V^u_R u_R, \tag{20a}$$

$$\hat{d}_L = V^d_L d_L, \qquad \hat{d}_R = V^d_R d_R. \tag{20b}$$

Finally, let us have a look at the gauge LQ interactions. Like in previous sections, we assume that ν_R are heavy due to the inverse seesaw [5,71] and therefore their interactions with the U_1 leptoquark are unimportant for the low-energy phenomenology. Interactions of U_1 with the other fermions can be rewritten as follows:

$$\begin{aligned} \mathcal{L} &= \frac{g_4}{\sqrt{2}} (\overline{q_L}\gamma^\mu {}^4\ell_L + \overline{d_R}\gamma^\mu {}^4e_R) U_{1\mu} + \text{H.c.} \\ &= \frac{g_4}{\sqrt{2}} \left[(\,\overline{\hat{q}_L} \quad 0\,)\gamma^\mu \begin{pmatrix} V^d_L & 0 \\ 0 & \mathbb{1} \end{pmatrix} (V^e_L)^\dagger \begin{pmatrix} \hat{\ell}_L \\ L_L \end{pmatrix} \right. \\ &\quad \left. + (\,\overline{\hat{d}_R} \quad 0\,)\gamma^\mu \begin{pmatrix} V^d_R & 0 \\ 0 & \mathbb{1} \end{pmatrix} (V^e_R)^\dagger \begin{pmatrix} \hat{e}_R \\ E_R \end{pmatrix} \right] U_{1_\mu} + \text{H.c.} \\ &= \frac{g_4}{\sqrt{2}} \left[(\,\overline{\hat{q}_L} \quad 0\,)\gamma^\mu (V_L) \begin{pmatrix} \hat{\ell}_L \\ L_L \end{pmatrix} \right. \\ &\quad \left. + (\,\overline{\hat{d}_R} \quad 0\,)\gamma^\mu (V_R) \begin{pmatrix} \hat{e}_R \\ E_R \end{pmatrix} \right] U_{1\mu} + \text{H.c.} \end{aligned} \tag{21}$$

The L_L field on the last line is the heavy $SU(2)_L$ doublet containing E_L as a component. Apparently, the novelty of such extended $SU(4)_C$ models consists in the fact that the unitary matrices $V_{L,R}$, defined by the last line of Eq. (21), are now of dimension $3 + k_{L,R}$. Using the block-form notation

$$V_{L,R} = \begin{pmatrix} V^0 & V^{\rm I} \\ V^{\rm II} & V^{\rm III} \end{pmatrix}_{L,R}, \tag{22}$$

only the 3×3 submatrices $V^0_{L,R}$ are relevant for the interactions among the SM fermions. The larger the numbers $k_{L,R}$ of extra lepton generations, the more parametric freedom in $V^0_{L,R}$ is available. With $k_L = k_R = 3$, one can already choose any form of $\frac{g_4}{m_{U_1}} V^0_{L,R}$, which is all that is relevant for the low-energy phenomenology at the leading order, cf. Eq. (13).

Similar models have already been studied in the literature, usually considering the cases equivalent to $(k_L, k_R) = (3,0)$ [72], (0,3) [55] or (3,3) [54]. In this work, we focus on the more economical models with $k_{L,R} < 3$, which are less challenging if one aims to capture all the possible NP signals in the model, but more restrictive if parameters leading to a chosen signal (such as the $b \to s\mu\mu$ anomalies) are searched for.

Note that enlarging the dimension of $V_{L,R}$ is indeed the only practical consequence of extending the theory of QLU from previous sections; we assume that the extra leptons are too heavy to be observed and ignore the details of the scalar sector responsible for the mixing. A construction of the scalar sector leading to a chosen form of $V_{L,R}$ in similar models can be found, e.g., in Ref. [63].

Note that although we keep neglecting the Z' in the model, it may actually be relevant in some cases. The discussion of this issue is deferred to Appendix B.

B. First signals of gauge leptoquark in extended $SU(4)_C$ models

We have performed an analysis similar to that described in Sec. III for the extended $SU(4)_C$ models with $(k_L, k_R) = (1,0), (0,1), (2,0), (0,2)$, and (1,1). Some details about the scanning procedure can be found in Appendix C.

With growing number of free parameters, more couplings can be "rotated away" from $V^0_{L,R}$ to the other parts of $V_{L,R}$. New interaction patterns become allowed, with lower limits on m_{U_1}. Naturally, the catalog of the *first future signals* (the observables which currently constrain m_{U_1} for some form of $V_{L,R}$) grows with the growing dimensions of these unitary matrices. The results are captured in Table IV.

While a lot of effort has been spent to fully explore the parameter space in the cases $(k_L, k_R) = (1,0)$ or (0,1), the number of parameters for $k_L + k_R = 2$ is quite high and we admit that the corresponding lists in Table IV may not be complete.

C. Addressing neutral current B anomalies

During the last decade, several discrepancies in both charged-current and neutral-current B-meson decays have been reported [73–77]. Plenty new physics interpretations have been suggested (see, e.g., [8,78]), including the U_1 leptoquark. Achieving the setup form Eq. (4) is meaningless within our restricted model as it requires so low scale of $SU(4)_C$ symmetry breaking that neglecting the other BSM fields would be inadequate. Nevertheless, reasonable considerations can be made once only the accommodation of the neutral-current anomalies is sought for. These anomalies include the tests of lepton flavor universality

$$\mathrm{R}_{K^{(*)}} = \frac{\mathrm{BR}(B \to K^{(*)}\mu\mu)}{\mathrm{BR}(B \to K^{(*)}ee)} \tag{23}$$

with $\mathrm{R}^{\mathrm{exp}}_{K^{(*)}} < \mathrm{R}^{\mathrm{SM}}_{K^{(*)}} = 1$ (see Table V). Further measurements indicate that the NP effect is in the $b \to s\mu\mu$ channel [76,77].

In order to ascribe this effect to the gauge LQ, the elements $V_{Ls\mu}$ and $V_{Lb\mu}$ need to be non-negligible. To avoid the scalar-type operators $\mathcal{O}_{\ell edq}$ involving electrons or muons, which are responsible for the most severe constraints found in Sec. IV, $k_R = 2$ generations of extra leptonic $SU(2)_L$-singlets are required; the model with $\dim(V_L)=3$ and $\dim(V_R) = 5$ allows for the following setup:

$$V_L = \begin{pmatrix} 0 & 0 & e^{i\delta_L} \\ e^{i\delta_1}\cos\gamma & -e^{-i\delta_2}\sin\gamma & 0 \\ e^{i\delta_2}\sin\gamma & e^{-i\delta_1}\cos\gamma & 0 \end{pmatrix}, \quad V^0_R = \begin{pmatrix} 0 & 0 & 0 \\ 0 & 0 & 0 \\ 0 & 0 & e^{i\delta_R} \end{pmatrix}. \tag{24}$$

TABLE IV. Possible future first signals of the gauge LQ in extended $SU(4)_C$ models featuring k_L extra lepton doublets and k_R extra charged-lepton singlets. For a given cell, all observables from the cells above and to the left are implicitly assumed to be included. The ellipses indicate that the catalogs in the relevant cell might not be complete.

Model	$k_L = 0$, dim $V_L = 3$	$k_L = 1$, dim $V_L = 4$	$k_L = 2$, dim $V_L = 5$
$k_R = 0$, dim $V_R = 3$	see Table I	$\mathrm{BR}(B^0 \to ee)$ $\mathrm{BR}(B_s \to ee)$ $(\varepsilon'/\varepsilon)_{K^0}$	$\mathrm{BR}(B^+ \to K^+\mu^+e^-)$ $\mathrm{BR}(B^+ \to K^+\mu^-e^+)$ ε_{K^0} …
$k_R = 1$, dim $V_R = 4$	$\mathrm{BR}(B^0 \to ee)$ $\mathrm{BR}(B_s \to ee)$ $(\varepsilon'/\varepsilon)_{K^0}$	ε_{K^0} …	
$k_R = 2$, dim $V_R = 5$	$\mathrm{BR}(B^+ \to K^+\mu^+e^-)$ $\mathrm{BR}(B^+ \to K^+\mu^-e^+)$ ε_{K^0} $R_{K^{(*)}}$ …		

TABLE V. Predictions for the benchmark case of Eqs. (24) and (25) for several observables with NP contribution.

Observable	Model prediction	Experiment	SM prediction
$R_K[(1.1;6)\ \mathrm{GeV}^2]$	0.79	0.85 ± 0.06 [73]	1.00 [79–81]
$R_{K^*}[(1.1;6)\ \mathrm{GeV}^2]$	0.79	0.68 ± 0.12 [74]	1.00 [81]
$\mathrm{BR}(B_s \to \mu^+\mu^-)$	3.2×10^{-9}	$(3.0 \pm 0.4) \times 10^{-9}$ [38]	$(3.7 \pm 0.2) \times 10^{-9}$ [FLAVIO]
$\mathrm{BR}(B^+ \to K^+\mu^+e^-)$	2.1×10^{-9}	$<6.4 \times 10^{-9}$ [82]	0
$\mathrm{BR}(B^+ \to K^+e^+\mu^-)$	2.1×10^{-9}	$<7.0 \times 10^{-9}$ [82]	0
$\mathrm{BR}(\mu \to e\gamma)$	1.9×10^{-13}	$<4.2 \times 10^{-13}$ [83]	0
$\mathrm{BR}(B^0 \to \tau^+\tau^-)$	9×10^{-7}	$<1.6 \times 10^{-3}$ [48]	2×10^{-8} [46]
$\mathrm{BR}(B_s \to e^\pm\tau^\mp)$	6.4×10^{-7}	N/A [38]	0
$\mathrm{BR}(B_s \to \mu^\pm\tau^\mp)$	6.4×10^{-7}	$<3.4 \times 10^{-5}$ [24]	0

Note that a similar pattern for V_L has been suggested in Ref. [55] and also in Ref. [59] within the $SU(4)_{C_L} \times SU(4)_{C_R} \times SU(2)_L \times U(1)_R$ framework where the couplings to the right-handed fermions are suppressed globally.

Adopting Eq. (24), the maximum likelihood fit is close to the simple case

$$\gamma = \pi/4, \quad \delta_1 = \delta_2 = \delta_L = \delta_R = 0, \quad m_{U_1} = 22\ \mathrm{TeV}, \tag{25}$$

which improves the global log-likelihood function of SMELLI [28] by more than 14 units compared to the SM, i.e. $\log(L/L^{\mathrm{SM}}) \approx 14$. Such a scenario accommodates well the $R_{K^{(*)}}$ anomaly and also significantly mitigates the tension in the additional $b \to s\mu\mu$ observables.

Using the standard normalization factor $\mathcal{N} = \frac{4G_F}{\sqrt{2}} V_{tb}V_{ts}^* \frac{e^2}{16\pi^2}$ for the effective four-fermion operators

$$\mathcal{O}_{9\_qq'll'} = \mathcal{N}(\overline{q'_L}\gamma_\mu q_L)(\overline{l'}\gamma^\mu l), \tag{26a}$$

$$\mathcal{O}_{10\_qq'll'} = \mathcal{N}(\overline{q'_L}\gamma_\mu q_L)(\overline{l'}\gamma^\mu \gamma_5 l) \tag{26b}$$

in the weak effective theory at the 5 GeV scale, Eqs. (24) (25) imply the following contributions of new physics to the wilson coefficients:

$$C^{\mathrm{NP}}_{9\_bs\mu\mu} = +C^{\mathrm{NP}}_{9\_bs\mu e} = -0.24, \tag{27a}$$

$$C^{\mathrm{NP}}_{9\_bsee} = C^{\mathrm{NP}}_{9\_bse\mu} = +0.24, \tag{27b}$$

$$C^{\mathrm{NP}}_{10\_bsll'} = -C^{\mathrm{NP}}_{9\_bsll'}. \tag{27c}$$

In comparison, the benchmark one-dimensional effective scenario with only $C^{\mathrm{NP}}_{9\_bs\mu\mu} = -C^{\mathrm{NP}}_{10\_bs\mu\mu} = -0.53$ [8] improves log-likelihood to $\log(L/L^{\mathrm{SM}}) = 18$; the simplified vector LQ setup in Eq. (4) leads to $\log(L/L^{\mathrm{SM}}) = 30$ as it also accommodates $R_{D^{(*)}}$. Note that the discussion in terms of confidence levels would be pointless since these models differ in number of free parameters.

Predictions for several important observables following from Eqs. (24) and (25) are given in Table V. As outlined in Sec. III B, the LQ has been integrated out at the tree level and the calculated LFV dipole operators responsible for $\mu \to e\gamma$ arise solely from the one-loop RGE running of the wilson coefficients. Thus, the predictions for the loop processes should be interpreted with caution.

In the scenarios with nonzero couplings V_{Lse}, V_{Lbe}, $V_{Ls\mu}$, and $V_{Lb\mu}$, the strongest bounds arise from $B^+ \to K^+\mu^\pm e^\mp$ and from the LFV loop processes like $\mu \to e\gamma$ (see Ref. [84] for a dedicated study). Generally, the constraints from the latter are quite strong. However, in the chiral leptoquark models with unitary interaction matrix, $\mu \to e\gamma$ is suppressed by an analog of the GIM mechanism. As the only nonvanishing element of V_R^0 in (24) is essentially irrelevant for $\mu \to e\gamma$, the same applies also to our case. Note that Ref. [84] did not consider the subleading terms and hence found exactly zero contributions to $\mu \to e\gamma$ for the case $V_{Lse}V^*_{Ls\mu} = -V_{Lbe}V^*_{Lb\mu}$. Reference [59] considered the case equivalent to V_L from (24) and $V_R = 0$, finding the constraint $m_{U_1} > 10$ TeV based on the *BABAR* search [85] for $B \to Ke\mu$. The very recent measurement by LHCb [82] has pushed this limit to 17 TeV for the considered interaction pattern.

Finally, let us note that although the Z' interactions are not lepton flavor universal, the couplings in the particular case of Eq. (24) are lepton flavor diagonal and, hence, the Z' does not mediate any flavor-violating processes (see Appendix A for more details about lepton flavor). At the same time, with the mass around 20 TeV, Z' is also safely hidden to the high-energy searches at LHC. We elaborate on Z' in Appendix B.

To conclude, the interactions of the $SU(4)_C$ gauge leptoquark in a model with two extra weak-isosinglet charged leptons can accommodate the neutral-current B-meson anomalies to a large extent. The suggested scenario can be excluded by future negative searches for $B \to Ke\mu$ at LHCb or Belle II.

VI. CONCLUSIONS

We have studied the phenomenology of the gauge leptoquark model with $SU(4)_C$ symmetry of the Pati-Salam type, taking into account the most recent experimental data. The catalog consisting of 11 observables which currently set the border of the excluded part of the parameter space has been compiled in Table I. These observables have a potential to uncover the gauge LQ signal even with a small improvement of the experimental sensitivity.

For the decays $P^0 \to l^+ l'^-$ not listed in the catalog, we have found the future experimental bounds needed in order to further probe the considered model.

Furthermore, we have explored a class of $SU(4)_C$ models with extra heavy vector-like leptons and searched for additional possible future first signals of the gauge LQ. We have also found the smallest of these models capable of accommodating the neutral current anomalies in B decays and identified the key future measurement which can exclude such a setup.

ACKNOWLEDGMENTS

We acknowledge the support from the Grant agency of the Czech Republic, Project No. 20-17490S, from the Grant Agency of Charles University (GAUK) Project No. 12481/2019, and from the Charles University Research Center UNCE/SCI/013. We would like to express our gratitude to Michal Malinský for his valuable advice and all the support.

APPENDIX A: GROUP THEORY OF LEPTON FLAVOR IN LEPTOQUARK MODELS

For simplicity, let us define the lepton flavor group in a wider sense as the $U(3)_{\rm LF}$ group acting uniformly by its defining representation on both SM leptonic triplets

$$\hat{e}_R = \begin{pmatrix} e \\ \mu \\ \tau \end{pmatrix}_R \quad \text{and} \quad \hat{\ell}_L = \begin{pmatrix} \ell_e \\ \ell_\mu \\ \ell_\tau \end{pmatrix}_L . \tag{A1}$$

Note that we have ignored the axial factor of what is usually called the lepton flavor group. There are three important subgroups of $U(3)_{\rm LF}$:

(1) The lepton number group is the Abelian factor emerging in the factorization $U(3)_{\rm LF} = SU(3)_{\rm LF} \times U(1)_{\mathcal{L}}$. It acts on $\hat{e}_R$ and $\hat{\ell}_L$ as multiplication by an overall complex phase.

(2) The lepton flavor group in the strict sense $U(1)^2_{\rm LF} = U(1)_{\mathcal{L}_\mu - \mathcal{L}_e} \times U(1)_{\mathcal{L}_\tau - \mathcal{L}_e} \subset SU(3)_{\rm LF}$ is a group of diagonal special unitary 3×3 matrices. In combination with the $\mathcal{L}$ conservation, the $U(1)^2_{\rm LF}$ symmetry would imply conservation of the individual lepton family numbers, satisfying $\mathcal{L}_e + \mathcal{L}_\mu + \mathcal{L}_\tau = \mathcal{L}$. Notice that despite various conventions for what is called the lepton flavor group, the term lepton-flavor violation (LFV) is being used strictly in relation with $U(1)^2_{\rm LF}$.

(3) Inspecting nondiagonal parts of the anticipated approximate LF symmetry consists especially in testing the lepton flavor universality (LFU) which can be associated with the group of permutation matrices $(S_3)_{\rm LFU} \subset U(3)_{\rm LF}$.

Since neither $U(1)^2_{\rm LF}$ nor $(S_3)_{\rm LFU}$ is a subgroup of the other, LFV does not necessarily imply LFU violation (LFUV) nor vice versa.

Let us trace the fate of these would-be symmetries in leptoquark interactions. For clarity of expression, consider only a single term, say $\overline{\hat{d}_R} \not{U}_1 V_R \hat{e}_R$; the generalization to full-fledged interaction such as those in Eq. (2) is straightforward.

(1) Apparently, the LQ interaction with the leptons and quarks conserves the lepton number $\mathcal{L}$ regardless of the form of the interaction matrix V_R, provided the U_1 leptoquark carries $\mathcal{L} = -1$.

(2) If two columns of the interaction matrix V_R are zero, then the LQ can be ascribed the corresponding flavor number ($\mathcal{L}_e$, $\mathcal{L}_\mu$ or $\mathcal{L}_\tau$) and there is no LFV. In the case V_R has a single zero column, only a one-dimensional subgroup of $U(1)^2_{\rm LF}$ is a symmetry of the interaction (only the noninteracting flavor remains preserved). If all its columns are nonempty, $U(1)^2_{\rm LF}$ is completely explicitly broken.

(3) On the other hand, respecting the $(S_3)_{\rm LFU}$ symmetry requires that all three columns of V_R are equal. Thus, the leptoquark brings new sources of LFUV whenever (at least) two columns of V_R differ.

These observations hold generally, for any kind of LQ and its interaction matrix. In principle, the form of the interaction matrices may be such that either $U(1)^2_{\rm LF}$ or $(S_3)_{\rm LFU}$ is an exact symmetry of the LQ interactions.

However, in the particular case of the gauge LQ in quark-lepton unification, the interaction matrix V_R is a subject of the unitarity conditions: the column normalization rule implies that none of the columns can be empty, the $U(1)^2_{\rm LF}$ symmetry is completely broken and the LQ inevitably mediates LFV processes. Complementarily, the column orthogonality condition implies violation of $(S_3)_{\rm LFU}$.

In fact, no nontrivial subgroup of $SU(3)_{\rm LF}$ can be a symmetry of $\overline{\hat{d}_R} \not{U}_1 V_R \hat{e}_R$ for any invertable (e.g., unitary) V_R: assuming $X \in U(3)_{\rm LF}$ acts as $\hat{e}_R \to X \hat{e}_R$ and $U_1 \to e^{i\varphi(X)} U_1$, the considered interaction remains intact if and only if $e^{i\varphi(X)} V_R X = V_R$, i.e., if X is a mere phase.

APPENDIX B: THE Z' BOSON IN $SU(4)_C$ MODELS

The features of the Z' boson can be reviewed most naturally when the intermediate gauge symmetry stage

$$G_{3121} = SU(3)_C \times U(1)_{[B-L]} \times SU(2)_L \times U(1)_R \tag{B1}$$

TABLE VI. Scheme of the sequential symmetry breaking in the quark-lepton symmetry scenarios. For each step, the corresponding branching rules, matching equations and gauge bosons which remain massless are specified.

G_{421}		$\mathrm{SU}(4)_C$	$U(1)_R$	$\mathrm{SU}(2)_L$
	$T_C^{1,\ldots,8}$	$[B-L]=\sqrt{\frac{8}{3}}T_C^{15}$		
$\downarrow$	$g_3=g_4$	$g_{BL}=\sqrt{\frac{3}{8}}g_4$		
	$G_\mu^{1,\ldots,8}=A_\mu^{1,\ldots,8}$	A_μ^{15}		
G_{3121}	$\mathrm{SU}(3)_C$	$U(1)_{[B-L]}$	$U(1)_R$	$\mathrm{SU}(2)_L$
		$Y=\frac{1}{2}[B-L]+R$		
$\downarrow$		$g'=\frac{g_{BL}g_R}{\sqrt{g_{BL}^2+(g_R/2)^2}}=2g_{BL}\sin\theta'$		
		$B_\mu=\sin\theta' A_\mu^{15}+\cos\theta' B'_\mu$		
G_{SM}		$U(1)_Y$		$\mathrm{SU}(2)_L$
		$Q=T_L^3+Y$		
$\downarrow$		$e=\frac{gg'}{\sqrt{g^2+g'^2}}=g\sin\theta_W$		
		$A_\mu=\cos\theta_W B_\mu-\sin\theta_W W_\mu^3$		
G_{vac}		$U(1)_Q$		

is considered. The details of the sequential breaking of the G_{421} symmetry including this step are summarized in Table VI.

In the first step of symmetry breaking, the $SU(4)_C$ factor is spontaneously broken at some high scale, way above the electroweak one, which (unlike for GUTs) can be chosen arbitrarily since our framework unifies the fermions but not the gauge interactions. The smallest possible first step of the $SU(4)_C$ breaking is

$$SU(4)_C \to SU(3)_C \times U(1)_{[B-L]}. \tag{B2}$$

The Abelian factor in Eq. (B2) is generated by

$$T_C^{15}=\frac{1}{2\sqrt{6}}\begin{pmatrix}\mathbb{1}_{3\times3} & 0\\ 0 & -3\end{pmatrix}. \tag{B3}$$

Quite commonly, its multiple

$$[B-L]=\sqrt{\frac{8}{3}}T_C^{15}=\mathrm{diag}(⅓,⅓,⅓,-1) \tag{B4}$$

is being used instead, which is compensated by redefinition of the gauge coupling, $g_{BL}=\sqrt{3/8}g_4$.

The name of the $[B-L]$ generator is motivated by its action on the unified fermionic representations in Eq. (1). However, one must keep in mind that action of this symmetry generator in Eq. (B4) does not necessarily coincide with the difference between the baryon number $\mathcal{B}$ and lepton number $\mathcal{L}$ for other fields in the model. For example, in the minimal quark-lepton symmetry model [3], both $\mathcal{B}$ and $\mathcal{L}$ are perturbatively conserved to all orders while T_C^{15} is spontaneously broken. Next, the extended models studied in Sec. V contain leptonic fields ${}^1\ell$ and ${}^1e$ which transform trivially under $SU(4)_C$ and hence also under $U(1)_{[B-L]}$. To emphasize the distinction between $\mathcal{B}-\mathcal{L}$ and the gauge symmetry generator (B4), we shall keep the square brackets around the latter in order to indicate that $[B-L]$ is an indivisible symbol.

The 19 gauge fields of the model can be cast as follows:

$$SU(4)_C\colon\ \mathcal{A}_\mu=\begin{pmatrix}G_\mu+\frac{1}{2\sqrt{6}}A_\mu^{15} & U_{1\mu}/\sqrt{2}\\ U_{1\mu}^\dagger/\sqrt{2} & -\frac{3}{2\sqrt{6}}A_\mu^{15}\end{pmatrix}, \tag{B5a}$$

$$SU(2)_L\colon\ \mathcal{W}_\mu=\frac{1}{2}\begin{bmatrix}W_\mu^3 & \sqrt{2}W_\mu^+\\ \sqrt{2}W_\mu^- & -W_\mu^3\end{bmatrix}, \tag{B5b}$$

$$U(1)_R\colon\ B'_\mu. \tag{B5c}$$

In Eq. (B5), the $(3+1)\times(3+1)$ block notation has been used. Together with the gluons G and charged intermediate vector bosons $W^\pm$, one can easily identify the vector leptoquark U_1. Furthermore, the three electrically neutral fields A^{15}, B', and W^3 mix into the photon, the Z boson, and to Z'.

The symmetry breaking (B2) gives mass only to the gauge leptoquark; the Z' boson acquires mass no sooner than during the second step,

$$U(1)_{[B-L]}\times U(1)_R \to U(1)_Y. \tag{B6}$$

Thus, while the precise ratio of $m_{U_1}/m_{Z'}$ depends on the scalar sector of the model, Z' can never be much heavier than U_1.

The rotation of the electrically neutral gauge fields to the mass basis can be written as

$$\begin{aligned}\begin{pmatrix}A_\mu^{15}\\ B'_\mu\\ W_\mu^3\end{pmatrix}&=\begin{pmatrix}\cos\theta' & \sin\theta' & 0\\ -\sin\theta' & \cos\theta' & 0\\ 0 & 0 & 1\end{pmatrix}\begin{pmatrix}\check{Z}'_\mu\\ B_\mu\\ W_\mu^3\end{pmatrix}\\ &=\begin{pmatrix}\cos\theta' & \sin\theta' & 0\\ -\sin\theta' & \cos\theta' & 0\\ 0 & 0 & 1\end{pmatrix}\begin{pmatrix}1 & 0 & 0\\ 0 & \cos\theta_W & \sin\theta_W\\ 0 & -\sin\theta_W & \cos\theta_W\end{pmatrix}\\ &\quad\times\begin{pmatrix}\cos\theta_m & \sin\theta_m & 0\\ -\sin\theta_m & \cos\theta_m & 0\\ 0 & 0 & 1\end{pmatrix}\begin{pmatrix}Z'_\mu\\ Z_\mu\\ A_\mu\end{pmatrix},\end{aligned} \tag{B7}$$

where $\tan\theta'=g_R/(2g_{BL})$ at the relevant scale, and θ_W is the weak mixing angle (see Table VI). The angle θ_m is very small when the symmetry breaking (B6) occurs way above the electroweak energy scale [3]. Hence, in the limit $m_{Z'}/m_Z\to\infty$, the Z' boson is given by

$$Z'_\mu = A^{15}_\mu \cos\theta' - B'_\mu \sin\theta'. \tag{B8}$$

and the Z' coupling can be obtained by rewriting the relevant terms in the covariant derivative using relations from Table VI,

$$g_{BL}[B-L]A^{15}_\mu + g_R R B'_\mu = g' Y B_\mu + \frac{g_{BL}}{\cos\theta'}([B-L] - 2Y\sin^2\theta')Z'_\mu, \tag{B9}$$

which is an analog to the SM case

$$g' Y B_\mu + g T^3_L W^3_\mu = eQA_\mu + \frac{g}{\cos\theta_w}(T^3_L - Q\sin^2\theta_w)Z_\mu. \tag{B10}$$

In the models of QLU, where all the fermions arise from $SU(4)_C$ quadruplets, the Z' interactions with both quarks and leptons are flavor-diagonal and universal, i.e., they respect the entire $U(3)_{\rm LF}$ symmetry. The coupling strength is governed by Eq. (B9). With the $SU(4)_C$ breaking scale around 100 TeV or higher, the resulting flavor-conserving 4-fermion operators are safely negligible in the simplest situations without the optional symmetry-breaking step of Eq. (B2). On the other hand, the role of Z' in the extended models might be much more important since the mass limits are generally lower and its interactions with the leptons do not necessarily conserve flavor.

Lepton-flavor conserving effective semileptonic interactions mediated by Z' could interfere with the SM amplitudes in the $q\bar{q} \xrightarrow{Z^*, Z'^*} l^+ l^-$ production in the $s \gg m_Z^2$ kinematic region. NP contributions to these processes are constrained by the high-p_T dilepton spectra measurements by Atlas and CMS, leading to limits around $m_{Z'} > 5$ TeV (depending on the Z' coupling assumed) [86,87]. As noted in Ref. [60], these limits also indirectly constrain the mass of the gauge LQ. This bound is important in models accommodating the anomalous value of R_D which require $m_{U_1} \sim 2$ TeV.

Reference [60] further states that "*the couplings of the Z' to SM fermions are necessarily flavor universal*" and "*proportional to the identity matrix in flavor space*" even in the models with extra fermions because the relevant charged lepton mixing "*necessarily involve states with the same $B-L$ charge*". This is, however, a misconception arising from not distinguishing between the gauge symmetry generator $[B-L]$ and the difference of the accidental global symmetries $\mathcal{B} - \mathcal{L}$. All the fermionic fields ${}^4\ell_L, {}^4e_R, {}^1\ell_{L,R}, {}^1e_{L,R}$ are fully justified to be called leptons and carry the lepton number $\mathcal{L}$, which is conserved by the gauge interactions. On the other hand, only the fields ${}^4\ell_L$ and ${}^4e_L$, which stem from $SU(4)_C$ quadruplets, are also charged with respect to $[B-L]$, the diagonal generator of the $SU(4)_C$ group. As a consequence of this, rotating the left-handed ($[B-L] - 2Y\sin^2\theta'$) lepton currents into the mass basis [see Eq. (21)] yields

$$\begin{aligned}(\overline{{}^4\ell_L} \quad \overline{{}^1\ell_L})&\begin{pmatrix} -1+\sin^2\theta' & 0 \\ 0 & \sin^2\theta' \end{pmatrix}\gamma^\mu \begin{pmatrix} {}^4\ell_L \\ {}^1\ell_L \end{pmatrix} \\ &= (\overline{\hat{\ell}_L} \quad \overline{L_L}) V^e_L \begin{pmatrix} -1+\sin^2\theta' & 0 \\ 0 & \sin^2\theta' \end{pmatrix} V^{e\dagger}_L \gamma^\mu \begin{pmatrix} \hat{\ell}_L \\ L_L \end{pmatrix}\end{aligned} \tag{B11a}$$

and similarly for the right-handed currents:

$$\begin{aligned}(\overline{{}^4e_R} \quad \overline{{}^1e_R})&\begin{pmatrix} -1+2\sin^2\theta' & 0 \\ 0 & 2\sin^2\theta' \end{pmatrix}\gamma^\mu \begin{pmatrix} {}^4e_R \\ {}^1e_R \end{pmatrix} \\ &= (\overline{\hat{e}_R} \quad \overline{E_R}) V^e_R \begin{pmatrix} -1+2\sin^2\theta' & 0 \\ 0 & 2\sin^2\theta' \end{pmatrix} V^{e\dagger}_R \gamma^\mu \begin{pmatrix} \hat{e}_R \\ E_R \end{pmatrix}.\end{aligned} \tag{B11b}$$

Finally, using the implicit definition of $V_{L,R}$ in Eq. (21) and the block notation of Eq. (22), one arrives to the following formula for the Z' couplings with the SM fermions:

$$\begin{aligned}\mathcal{L}^{Z'll} = \frac{g_{BL}}{\cos\theta'}\Big[&\overline{\hat{\ell}}_{Li}(s'^2\mathbb{1} - (V^0_L)^\dagger V^0_L)\gamma^\mu \hat{\ell}_L{}^i \\ &+ \overline{\hat{e}}_R(2s'^2\mathbb{1} - (V^0_R)^\dagger V^0_R)\gamma^\mu \hat{e}_R \\ &+ \frac{1+s'^2}{3}\overline{\hat{q}}_{Li}\gamma^\mu \hat{q}_L{}^i + \frac{1-4s'^2}{3}\overline{\hat{u}}_R\gamma^\mu \hat{u}_R \\ &+ \frac{1+2s'^2}{3}\overline{\hat{d}}_R\gamma^\mu \hat{d}_R\Big]Z'_\mu,\end{aligned} \tag{B12}$$

where $s'^2 \equiv \sin^2\theta'$ amounts to 0.08 at the 2 TeV scale or to $s'^2 \simeq 0.12$ in the 200 TeV ballpark (assuming SM-like gauge coupling running up to $m_{Z'}$). Thus, the Z' interactions with leptons in the extended $SU(4)_C$ models are not necessarily flavor universal and, in general, the diagonal couplings could actually be strongly suppressed.

As a consequence, the limits on $m_{Z'}$ from the high-energy dilepton spectra may be considerably weakened for certain patterns of $V^0_{L,R}$. The simplified reasoning of Ref. [60] mentioned above has been used as a no-go argument for abandoning the models with the G_{421} gauge group and focusing on G_{4321}-based models instead when attempting to accommodate $\mathrm{R}_{D^{(*)}}$. In this respect, we note that achieving the form of $V^0_{L,R}$ from Eq. (4) in the framework of extended G_{421} models would imply that the Z' couplings to the e and μ leptons are suppressed. Since the $Z'^* \to \tau^+\tau^-$ channel is experimentally less constrained [88], a valid no-go argument needs to be more subtle. Nevertheless, the scenarios with the $SU(4)_C$-breaking scale as low as 2 TeV require full model specification since the effects of the new scalar and fermionic degrees of freedom would be important. This is far beyond the scope of this paper.

In any case, this study is focusing on the extended $SU(4)_C$ models with $k_L + k_R \leq 2$. Such frameworks can not accommodate the $R_{D^{(*)}}$ anomalies even if the Z' is completely ignored due to the residual constraints on the leptoquark interaction matrices $V^0_{L,R}$ from the unitarity of $V_{L,R}$.

During scanning of the parameter space of these models, we have not encountered a parameter point allowing for m_{U_1} smaller than 18 TeV. Since the models allow for a similarly heavy Z', the constraints from this field are not severe: unlike the gauge LQ, Z' does not contribute to the scalar-type 2-quark-2-lepton operators $\mathcal{O}_{\ell edq}$ but only to the wilson coefficients multiplying the vector-type ones $(\mathcal{O}_{ed}, \mathcal{O}_{\ell q})$ and further to those of flavor-conserving 4-lepton or 4-quark operators, all of which are experimentally less restricted.

In this analysis, the Z' contributions to the wilson coefficients are not calculated. Including them could be a part of a future study focusing on the extended $SU(4)_C$ models.

APPENDIX C: OPTIMIZING THE SCANNING PROCEDURE

The experimental data collected over the last decades provided rather stringent constraints on mass of the considered leptoquark. Some of the most restraining processes are the decays of $K^0_L \to l^+ l'^-$ and the $\mu \to e$ conversion on gold nuclei, see Table I. Here we identify areas in the parameter space in which these decays are suppressed, and thus allow for lighter leptoquark.

1. Avoiding $K^0_L \to l^+ l'^-$

The scanning procedure mentioned in Sec. III C is optimized when we restrict the parameter space to a subspace in which

$$\mathrm{BR}_V(K^0_L \to l l') = 0. \tag{C1}$$

Schematically, the V_L and V_R matrices read

$$\left(\begin{array}{ccc|c} V_{de} & V_{d\mu} & V_{d\tau} & \\ V_{se} & V_{s\mu} & V_{s\tau} & V^{\mathrm{I}} \\ V_{be} & V_{b\mu} & V_{b\tau} & \\ \hline & V^{\mathrm{II}} & & V^{\mathrm{III}} \end{array}\right)_{L,R}, \tag{C2}$$

where u, d, s are quarks, e, μ, τ are leptons and each element represents the strength of interaction of these two fermions with the leptoquark. The block matrices V^{I}, V^{II}, and V^{III} are present only in the extended models studied in Sec. V. As follows from Eqs. (9)–(12), the BR's of the leptonic K^0_L decays are proportional to

$$\beta^2_{K^0_L,e\mu} = \beta^2_{K^0_L,\mu e} = \frac{1}{2}|V_{Lde}V^*_{Rs\mu} + V_{Lse}V^*_{Rd\mu}|^2 + \frac{1}{2}|V_{Ld\mu}V^*_{Rse} + V_{Ls\mu}V^*_{Rde}|^2, \tag{C3a}$$

$$\beta^2_{K^0_L,ee} = |V_{Lde}V^*_{Rse} + V_{Lse}V^*_{Rde}|^2, \tag{C3b}$$

$$\beta^2_{K^0_L,\mu\mu} = |V_{Ld\mu}V^*_{Rs\mu} + V_{Ls\mu}V^*_{Rd\mu}|^2. \tag{C3c}$$

All these β's vanish if and only if

$$\begin{pmatrix} V_{Lde} & V_{Lse} \\ V_{Ld\mu} & V_{Ls\mu} \end{pmatrix} \begin{pmatrix} V_{Rs\mu} & V_{Rd\mu} \\ V_{Rse} & V_{Rde} \end{pmatrix}^* = \begin{pmatrix} 0 & 0 \\ 0 & 0 \end{pmatrix}. \tag{C4}$$

When we think of V_{Lql} as fixed numbers and V_{Rql} as the unknowns, the necessary condition for a nontrivial solution to exist shrinks to

$$\begin{vmatrix} V_{Lde} & V_{Ld\mu} \\ V_{Lse} & V_{Ls\mu} \end{vmatrix} = 0, \tag{C5}$$

where $|V|$ stands for determinant. On the other hand, we can treat V_{Rql} as fixed numbers and V_{Lql} as variables, which leads to analogous result for the V_R matrix. Hence, the determinants of the top left 2×2 submatrices of both V_L and V_R has to be equal to zero, regardless of the dimensionality of these matrices.

Now we use a simplified rule of Laplace expansion in multiple rows (as derived by Laplace in 1772, more on this e.g., [89])

$$|M^{-1}|_{IJ} = \pm \frac{|M|_{I'J'}}{|M|}, \tag{C6}$$

where $|M|_{IJ}$ is the IJ-minor, i.e., the determinant of the submatrix obtained from M by deleting rows and columns from sets $I, J \subset D = \{1, \ldots, \dim(M)\}$. The set I' (J') is the complement of I (J) in D, so that every row and every column index appears exactly once in Eq. (C6). If M is a unitary matrix, its determinant is just a complex phase, and we can further simplify Eq. (C6) to

$$\text{phase} \times |M|_{IJ} = |M|_{I'J'}. \tag{C7}$$

In other words, the determinant of any submatrix of a unitary matrix is equal in magnitude to the determinant of the complementary submatrix. Applying this observation to the V_L and V_R matrices of dimension 3, Eq. (C5) leads to

$$V_{Lb\tau} = V_{Rb\tau} = 0 \tag{C8}$$

with an implication $\mathrm{BR}_V(B^0_{d,s} \to \tau\tau) = 0$ [which has been derived also in Ref. [4] by directly solving Eqs. (C3) in a specific parametrization]. Note also that the "solutions" to the B anomalies which leave out the unitarity constrains such as Eq. (4), usually assume that the $V_{L,Rb\tau}$ elements are the largest ones in order to address also $\mathrm{R}_{D^{(*)}}$. Therefore, $\mathrm{R}_{D^{(*)}}$ can not be accommodated within the QLU model.

Fulfilling the rather simple condition (C5) can be tough for V_L, V_R of higher dimensions. To this end, we introduce the composite parametrization of $U(n)$ matrices [90,91], which turns out to be particularly convenient in this respect. Its n^2 parameters λ_{ij} consist of $\frac{1}{2}n(n-1)$ angles ($i < j$) and $\frac{1}{2}n(n+1)$ phases ($i \geq j$). A 3×3 matrix in this parametrization reads

$$\begin{pmatrix} c_{12}c_{13}e^{i\lambda_{11}} & (c_{23}s_{12} - c_{12}s_{13}s_{23}e^{i\lambda_{32}})e^{i\lambda_{22}} & (s_{12}s_{23} + c_{12}c_{23}s_{13}e^{i\lambda_{32}})e^{i\lambda_{33}} \\ -c_{13}s_{12}e^{i\lambda_{11}+i\lambda_{21}} & (c_{12}c_{23} + s_{12}s_{13}s_{23}e^{i\lambda_{32}})e^{i\lambda_{22}+i\lambda_{21}} & (c_{12}s_{23} - c_{23}s_{12}s_{13}e^{i\lambda_{32}})e^{i\lambda_{33}+i\lambda_{21}} \\ -s_{13}e^{i\lambda_{11}+i\lambda_{31}} & -c_{13}s_{23}e^{i\lambda_{22}+i\lambda_{31}+i\lambda_{32}} & c_{13}c_{23}e^{i\lambda_{31}+i\lambda_{32}+i\lambda_{33}} \end{pmatrix}. \tag{C9}$$

For higher dimensions we refer to the original literature [90,91] or to the publicly available implementation in Wolfram Mathematica [92].

The beautiful advantage of the composite parametrization is that the subspace obeying Eq. (C1) can be obtained by fixing the same parameters for *any dimension* ≥ 3 *of* V_L *and* V_R. The necessary condition (C5) for existence of the solution is fulfilled by

$$\lambda_{L23} = \lambda_{R23} = \frac{\pi}{2}. \tag{C10}$$

With this in hand, it can be shown that setting

$$\lambda_{L12} = -\lambda_{R12}, \tag{C11a}$$

$$\lambda_{L21} = -\lambda_{R21}, \tag{C11b}$$

solves Eqs. (C4) entirely. Naively, other solutions can be found but they fall outside the proper domain of the λ's. An equivalent solution to (C3) was found in Ref. [4] for $\dim V_L = \dim V_R = 3$ within a different parametrization.

2. Avoiding $\mathbf{CR}(\mu \to e, \mathbf{Au})$

Leaving the K^0_L decays for a while, we now focus on another very important constraint stemming from the limits on $\mu \to e$ conversion on gold nuclei, $\mathrm{CR}(\mu \to e, \mathrm{Au}) < 7 \times 10^{-13}$ [43]. In the same manner, we enforce

$$\mathrm{CR}(\mu \to e, \mathrm{Au}) = 0. \tag{C12}$$

A leptoquark with $Q = +⅔$ mediates this process at the tree level by an interaction with the d quarks and the sea s quarks in the nucleons. The calculation in FLAVIO is based on Ref. [93]. The scalar-type effective vertices, $(\overline{d_R}d_L)(\overline{e_L}\mu_R)$ and $(\overline{d_R}d_L)(\overline{\mu_L}e_R)$, are predicted to engage in this process even more efficiently than the vector-type ones. Thus, to avoid these constraints when searching for limits from other interesting processes, the following condition must be approximately fulfilled:

$$|V_{Lde}V^*_{Rd\mu}|^2 + |V_{Rde}V^*_{Ld\mu}|^2 = 0. \tag{C13}$$

It can be shown that any $V_{L,R}$ pair obeying (C13) together with the set of Eqs. (C3) must necessarily have some of the elements from the upper left 2×2 submatrix equal to zero. The possible patterns for $V_{L,R}$ are

$$V_L = \left(\begin{array}{cc|c} \bullet & 0 & \\ \bullet & 0 & \\ \hline & & \end{array}\right), \qquad V_R = \left(\begin{array}{cc|c} \bullet & 0 & \\ \bullet & 0 & \\ \hline & & \end{array}\right); \tag{C14a}$$

$$V_L = \left(\begin{array}{cc|c} 0 & \bullet & \\ 0 & \bullet & \\ \hline & & \end{array}\right), \qquad V_R = \left(\begin{array}{cc|c} 0 & \bullet & \\ 0 & \bullet & \\ \hline & & \end{array}\right); \tag{C14b}$$

$$V_L = \left(\begin{array}{cc|c} 0 & 0 & \\ \bullet & \bullet & \\ \hline & & \end{array}\right), \qquad V_R = \left(\begin{array}{cc|c} 0 & 0 & \\ \bullet & \bullet & \\ \hline & & \end{array}\right); \tag{C14c}$$

$$V_L = \left(\begin{array}{cc|c} 0 & 0 & \\ 0 & 0 & \\ \hline & & \end{array}\right), \qquad V_R = \left(\begin{array}{cc|c} \bullet & \bullet & \\ \bullet & \bullet & \\ \hline & & \end{array}\right); \tag{C14d}$$

$$V_L = \left(\begin{array}{cc|c} \bullet & \bullet & \\ \bullet & \bullet & \\ \hline & & \end{array}\right), \qquad V_R = \left(\begin{array}{cc|c} 0 & 0 & \\ 0 & 0 & \\ \hline & & \end{array}\right), \tag{C14e}$$

where • denotes an unfixed value. The last two cases are available only when V_L or V_R has dimension $n \geq 4$, respectively.

Finding the unitary parametrization fulfilling both Eqs. (C3) and (C13) is straightforward though somewhat tedious as the solution has to be found for each dimension of V_L and V_R separately.

Notable, but order-of-magnitude smaller, contributions to the coherent $\mu \to e$ conversion still arise from vector-type operators (triggered by $V_{Lde}V^*_{Ld\mu}$ and $V_{Rde}V^*_{Rd\mu}$) and well as the muon conversion on the sea s-quarks in the nucleons (such amplitudes are proportional to $V_{Lse}V^*_{Rs\mu}$ or $V_{Lse}V^*_{Rs\mu}$).

[1] J. C. Pati and A. Salam, Lepton number as the fourth color, Phys. Rev. D **10**, 275 (1974); **11**, 703(E) (1975).

[2] J. C. Pati, A. Salam, and U. Sarkar, $\Delta B = -\Delta L$, neutron $\to e^-\pi^+$, e^-K^+, $\mu^-\pi^+$ and μ^-K^+ decay modes in $SU(2)_L \times SU(2)_R \times SU(4)^{\mathrm{col}}$ or $SO(10)$, Phys. Lett. **133B**, 330 (1983).

[3] A. D. Smirnov, The minimal quark-lepton symmetry model and the limit on Z' mass, Phys. Lett. B **346**, 297 (1995).

[4] A. D. Smirnov, Vector leptoquark mass limits and branching ratios of $K_L^0, B^0, B_s \to l_i^+ l_j^-$ decays with account of fermion mixing in leptoquark currents, Mod. Phys. Lett. A **33**, 1850019 (2018).

[5] P. Fileviez Pérez and M. B. Wise, Low scale quark-lepton unification, Phys. Rev. D **88**, 057703 (2013).

[6] D. Ambrose *et al.* (BNL Collaboration), New Limit on Muon and Electron Lepton Number Violation from $K_L^0 \to \mu^\pm e^\mp$ Decay, Phys. Rev. Lett. **81**, 5734 (1998).

[7] J. Kumar, D. London, and R. Watanabe, Combined explanations of the $b \to s\mu^+\mu^-$ and $b \to c\tau^-\bar{\nu}$ anomalies: A general model analysis, Phys. Rev. D **99**, 015007 (2019).

[8] J. Aebischer, W. Altmannshofer, D. Guadagnoli, M. Reboud, P. Stangl, and D. M. Straub, B-decay discrepancies after Moriond 2019, Eur. Phys. J. C **80**, 252 (2020).

[9] G. Valencia and S. Willenbrock, Quark-lepton unification and rare meson decays, Phys. Rev. D **50**, 6843 (1994).

[10] A. V. Kuznetsov and N. V. Mikheev, Vector leptoquarks could be rather light?, Phys. Lett. B **329**, 295 (1994).

[11] A. D. Smirnov, Mass limits for scalar and gauge leptoquarks from $K_L^0 \to e^\mp\mu^\pm$, $B^0 \to e^\mp\tau^\pm$ decays, Mod. Phys. Lett. A **22**, 2353 (2007).

[12] A. V. Kuznetsov, N. V. Mikheev, and A. V. Serghienko, The third type of fermion mixing in the lepton and quark interactions with leptoquarks, Int. J. Mod. Phys. A **27**, 1250062 (2012).

[13] FLAVIO · flavour phenomenology in the Standard Model and beyond, https://flav-io.github.io (accessed 1.05.2020).

[14] P. Y. Popov and A. D. Smirnov, Rare t-quark decays $t \to c l_j^+ l_k^-$, $t \to c\tilde{\nu}_j \nu_k$ in the minimal four color symmetry model, Mod. Phys. Lett. A **20**, 755 (2005).

[15] P. Popov, A. V. Povarov, and A. D. Smirnov, Fermionic decays of scalar leptoquarks and scalar gluons in the minimal four color symmetry model, Mod. Phys. Lett. A **20**, 3003 (2005).

[16] A. V. Povarov and A. D. Smirnov, Limits on scalar-leptoquark masses from lepton-flavor-violating processes of the $l_i \to l_j\gamma$ type, Phys. At. Nucl. **74**, 732 (2011).

[17] I. V. Frolov, M. V. Martynov, and A. D. Smirnov, Resonance contribution of scalar color octet to $t\bar{t}$ production at the LHC in the minimal four-color quark–lepton symmetry model, Mod. Phys. Lett. A **31**, 1650224 (2016).

[18] C. Murgui and M. B. Wise, Scalar leptoquarks, baryon number violation, and Pati-Salam symmetry, Phys. Rev. D **104**, 035017 (2021).

[19] T. Faber, M. Hudec, M. Malinský, P. Meinzinger, W. Porod, and F. Staub, A unified leptoquark model confronted with lepton non-universality in B-meson decays, Phys. Lett. B **787**, 159 (2018).

[20] T. Faber, M. Hudec, H. Kolešová, Y. Liu, M. Malinský, W. Porod, and F. Staub, Collider phenomenology of a unified leptoquark model, Phys. Rev. D **101**, 095024 (2020).

[21] P. Fileviez Perez, C. Murgui, and A. D. Plascencia, Leptoquarks and matter unification: Flavor anomalies and the muon $g-2$, Phys. Rev. D **104**, 035041 (2021).

[22] P. Fileviez Perez and C. Murgui, Flavor anomalies and quark-lepton unification, Phys. Rev. D **106**, 035033 (2022).

[23] A. D. Smirnov (private communication).

[24] R. Aaij *et al.* (LHCb Collaboration), Search for the Lepton-Flavour-Violating Decays $B_s^0 \to \tau^\pm\mu^\mp$ and $B^0 \to \tau^\pm\mu^\mp$, Phys. Rev. Lett. **123**, 211801 (2019).

[25] J. Aebischer, J. Kumar, and D. M. Straub, Wilson: A python package for the running and matching of wilson coefficients above and below the electroweak scale, Eur. Phys. J. C **78**, 1026 (2018).

[26] Wilson, https://wilson-eft.github.io/ (accessed 1.05.2020).

[27] D. M. Straub, FLAVIO, a python package for flavour and precision phenomenology in the Standard Model and beyond, arXiv:1810.08132.

[28] J. Aebischer, J. Kumar, P. Stangl, and D. M. Straub, A global likelihood for precision constraints and flavour anomalies, Eur. Phys. J. C **79**, 509 (2019).

[29] SMELLI · A global likelihood for the Standard Model Effective Fields Theory, https://smelli.github.io (accessed 1.05.2020).

[30] J. Aebischer *et al.*, Wcxf: An exchange format for wilson coefficients beyond the Standard Model, Comput. Phys. Commun. **232**, 71 (2018).

[31] WCxf: An exchange format for WILSON coefficients beyond the Standard Model, https://wcxf.github.io/ (accessed 1.05.2020).

[32] M. Hudec, Aspects of baryon and lepton number non-conservation in the Standard model of particle interactions and beyond, Ph.D. thesis, Charles University, 2021, http://hdl.handle.net/20.500.11956/152370.

[33] SMELLI v2.1.1.1, 10.5281/zenodo.7814299.

[34] I. Doršner, S. Fajfer, A. Greljo, J. F. Kamenik, and N. Košnik, Physics of leptoquarks in precision experiments and at particle colliders, Phys. Rep. **641**, 1 (2016).

[35] D. Ambrose *et al.* (BNL E871 Collaboration), First Observation of the Rare Decay Mode $K_L^0 \to e^+e^-$, Phys. Rev. Lett. **81**, 4309 (1998).

[36] G. Valencia, Long distance contribution to $K_L \to \ell^+\ell^-$, Nucl. Phys. **B517**, 339 (1998).

[37] D. Gomez Dumm and A. Pich, Long Distance Contributions to the $K_L \to \mu^+\mu^-$ Decay Width, Phys. Rev. Lett. **80**, 4633 (1998).

[38] P. Zyla *et al.* (Particle Data Group), Review of particle physics, Prog. Theor. Exp. Phys. **2020**, 083C01 (2020).

[39] R. Aaij *et al.* (LHCb Collaboration), Constraints on the $K_S^0 \to \mu^+\mu^-$ Branching Fraction, Phys. Rev. Lett. **125**, 231801 (2020).

[40] G. D'Ambrosio and T. Kitahara, Direct CP Violation in $K \to \mu^+\mu^-$, Phys. Rev. Lett. **119**, 201802 (2017).

[41] R. Aaij *et al.* (LHCb Collaboration), Search for the lepton-flavour violating decays $\mathrm{B}_{(s)}^0 \to e^\pm\mu^\mp$, J. High Energy Phys. 03 (2018) 078.

[42] V. Cirigliano and I. Rosell, $\pi/K \to e\bar{\nu}_e$ branching ratios to $O(e^2p^4)$ in Chiral Perturbation Theory, J. High Energy Phys. 10 (2007) 005.

[43] W. H. Bertl *et al.* (SINDRUM II Collaboration), A search for muon to electron conversion in muonic gold, Eur. Phys. J. C **47**, 337 (2006).

[44] F. Ambrosino *et al.* (KLOE Collaboration), Search for the $K_S \to e^+e^-$ decay with the KLOE detector, Phys. Lett. B **672**, 203 (2009).
[45] R. Aaij *et al.* (LHCb Collaboration), Search for the Rare Decays $B_s^0 \to e^+e^-$ and $B^0 \to e^+e^-$, Phys. Rev. Lett. **124**, 211802 (2020).
[46] C. Bobeth, M. Gorbahn, T. Hermann, M. Misiak, E. Stamou, and M. Steinhauser, $B_{s,d} \to l^+l^-$ in the Standard Model with Reduced Theoretical Uncertainty, Phys. Rev. Lett. **112**, 101801 (2014).
[47] B. Aubert *et al.* (*BABAR* Collaboration), Searches for the decays $B^0 \to l^\pm\tau^\mp$ and $B^+ \to l^+\nu$ $(l = e, \mu)$ using hadronic tag reconstruction, Phys. Rev. D **77**, 091104 (2008).
[48] R. Aaij *et al.* (LHCb Collaboration), Search for the Decays $B_s^0 \to \tau^+\tau^-$ and $B^0 \to \tau^+\tau^-$, Phys. Rev. Lett. **118**, 251802 (2017).
[49] G. Isidori and R. Unterdorfer, On the short distance constraints from $K_{L,S} \to \mu^+\mu^-$, J. High Energy Phys. 01 (2003) 009.
[50] V. Chobanova, G. D'Ambrosio, T. Kitahara, M. Lucio Martinez, D. Martinez Santos, I. S. Fernandez, and K. Yamamoto, Probing SUSY effects in $K_S^0 \to \mu^+\mu^-$, J. High Energy Phys. 05 (2018) 024.
[51] W. Altmannshofer *et al.* (Belle-II Collaboration), The Belle II Physics Book, Prog. Theor. Exp. Phys. **2019**, 123C01 (2019); **2020**, 029201(E) (2020).
[52] S. Cunliffe, Prospects for rare B decays at Belle II, arXiv:1708.09423.
[53] D. Bečirević, O. Sumensari, and R. Zukanovich Funchal, Lepton flavor violation in exclusive $b \to s$ decays, Eur. Phys. J. C **76**, 134 (2016).
[54] L. Calibbi, A. Crivellin, and T. Li, Model of vector leptoquarks in view of the *B*-physics anomalies, Phys. Rev. D **98**, 115002 (2018).
[55] S. Balaji, R. Foot, and M. A. Schmidt, Chiral SU(4) explanation of the $b \to s$ anomalies, Phys. Rev. D **99**, 015029 (2019).
[56] J. Bernigaud, M. Blanke, I. de Medeiros Varzielas, J. Talbert, and J. Zurita, LHC signatures of τ-flavoured vector leptoquarks, J. High Energy Phys. 08 (2022) 127.
[57] S. Balaji and M. A. Schmidt, Unified SU(4) theory for the $R_{D^{(*)}}$ and $R_{K^{(*)}}$ anomalies, Phys. Rev. D **101**, 015026 (2020).
[58] N. Assad, B. Fornal, and B. Grinstein, Baryon number and lepton universality violation in leptoquark and diquark models, Phys. Lett. B **777**, 324 (2018).
[59] B. Fornal, S. A. Gadam, and B. Grinstein, Left-right SU(4) vector leptoquark model for flavor anomalies, Phys. Rev. D **99**, 055025 (2019).
[60] M. J. Baker, J. Fuentes-Martín, G. Isidori, and M. König, High-p_T signatures in vector–leptoquark models, Eur. Phys. J. C **79**, 334 (2019).
[61] B. Diaz, M. Schmaltz, and Y.-M. Zhong, The leptoquark Hunter's guide: Pair production, J. High Energy Phys. 10 (2017) 097.
[62] L. Di Luzio, A. Greljo, and M. Nardecchia, Gauge leptoquark as the origin of B-physics anomalies, Phys. Rev. D **96**, 115011 (2017).
[63] L. Di Luzio, J. Fuentes-Martin, A. Greljo, M. Nardecchia, and S. Renner, Maximal flavour violation: A Cabibbo mechanism for leptoquarks, J. High Energy Phys. 11 (2018) 081.
[64] A. Greljo and B. A. Stefanek, Third family quark–lepton unification at the TeV scale, Phys. Lett. B **782**, 131 (2018).
[65] C. Cornella, J. Fuentes-Martin, and G. Isidori, Revisiting the vector leptoquark explanation of the B-physics anomalies, J. High Energy Phys. 07 (**2019**) 168.
[66] M. Bordone, C. Cornella, J. Fuentes-Martín, and G. Isidori, Low-energy signatures of the PS^3 model: From *B*-physics anomalies to LFV, J. High Energy Phys. 10 (2018) 148.
[67] M. Fernández Navarro and S. F. King, *B*-anomalies in a twin Pati-Salam theory of flavour, J. High Energy Phys. 02 (2023) 188.
[68] R. Barbieri, G. Isidori, A. Pattori, and F. Senia, Anomalies in *B*-decays and $U(2)$ flavour symmetry, Eur. Phys. J. C **76**, 67 (2016).
[69] R. Barbieri, C. W. Murphy, and F. Senia, B-decay anomalies in a composite leptoquark model, Eur. Phys. J. C **77**, 8 (2017).
[70] R. Barbieri and A. Tesi, *B*-decay anomalies in Pati-Salam SU(4), Eur. Phys. J. C **78**, 193 (2018).
[71] R. N. Mohapatra, Mechanism for Understanding Small Neutrino Mass in Superstring Theories, Phys. Rev. Lett. **56**, 561 (1986).
[72] R. Foot, An alternative $SU(4) \otimes SU(2)_L \otimes SU(2)_R$ model, Phys. Lett. B **420**, 333 (1998).
[73] R. Aaij *et al.* (LHCb Collaboration), Search for Lepton-Universality Violation in $B^+ \to K^+\ell^+\ell^-$ Decays, Phys. Rev. Lett. **122**, 191801 (2019).
[74] R. Aaij *et al.* (LHCb Collaboration), Test of lepton universality with $B^0 \to K^{*0}\ell^+\ell^-$ decays, J. High Energy Phys. 08 (2017) 055.
[75] Y. S. Amhis *et al.* (HFLAV Collaboration), Averages of b-hadron, c-hadron, and τ-lepton properties as of 2018, Eur. Phys. J. C **81**, 226 (2021).
[76] R. Aaij *et al.* (LHCb Collaboration), Differential branching fractions and isospin asymmetries of $B \to K^{(*)}\mu^+\mu^-$ decays, J. High Energy Phys. 06 (2014) 133.
[77] R. Aaij *et al.* (LHCb Collaboration), Angular analysis of the $B^0 \to K^{*0}\mu^+\mu^-$ decay using 3 fb^{-1} of integrated luminosity, J. High Energy Phys. 02 (2016) 104.
[78] W. Altmannshofer and P. Stangl, New physics in rare B decays after Moriond 2021, Eur. Phys. J. C **81**, 952 (2021).
[79] G. Isidori, D. Lancierini, S. Nabeebaccus, and R. Zwicky, QED in $\bar{B} \to \bar{K}\ell^+\ell^-$ LFU ratios: Theory versus experiment, a Monte Carlo study, J. High Energy Phys. 10 (2022) 146.
[80] G. Isidori, S. Nabeebaccus, and R. Zwicky, QED corrections in $\bar{B} \to \bar{K}\ell^+\ell^-$ at the double-differential level, J. High Energy Phys. 12 (2020) 104.
[81] M. Bordone, G. Isidori, and A. Pattori, On the Standard Model predictions for R_K and R_{K^*}, Eur. Phys. J. C **76**, 440 (2016).
[82] R. Aaij *et al.* (LHCb Collaboration), Search for Lepton-Flavor Violating Decays $B^+ \to K^+\mu^\pm e^\mp$, Phys. Rev. Lett. **123**, 241802 (2019).
[83] A. M. Baldini *et al.* (MEG Collaboration), Search for the lepton flavour violating decay $\mu^+ \to \mathrm{e}^+\gamma$ with the full dataset of the MEG experiment, Eur. Phys. J. C **76**, 434 (2016).

[84] A. Crivellin, D. Müller, A. Signer, and Y. Ulrich, Correlating lepton flavor universality violation in B decays with $\mu \to e\gamma$ using leptoquarks, Phys. Rev. D **97**, 015019 (2018).
[85] B. Aubert *et al.* (*BABAR* Collaboration), Measurements of branching fractions, rate asymmetries, and angular distributions in the rare decays $B \to K\ell^+\ell^-$ and $B \to K^*\ell^+\ell^-$, Phys. Rev. D **73**, 092001 (2006).
[86] M. Aaboud *et al.* (ATLAS Collaboration), Search for new high-mass phenomena in the dilepton final state using 36 fb^{-1} of proton-proton collision data at $\sqrt{s} = 13$ TeV with the ATLAS detector, J. High Energy Phys. 10 (2017) 182.
[87] A. M. Sirunyan *et al.* (CMS Collaboration), Search for high-mass resonances in dilepton final states in proton-proton collisions at $\sqrt{s} = 13$ TeV, J. High Energy Phys. 06 (2018) 120.
[88] M. Aaboud *et al.* (ATLAS Collaboration), Search for additional heavy neutral Higgs and gauge bosons in the ditau final state produced in 36 fb^{-1} of pp collisions at $\sqrt{s} = 13$ TeV with the ATLAS detector, J. High Energy Phys. 01 (2017) 055.
[89] V. Prasolov and S. Ivanov, *Problems and Theorems in Linear Algebra*, Translations of Mathematical Monographs, Vol. 134 (American Mathematical Society, Providence, 1994).
[90] C. Spengler, M. Huber, and B. C. Hiesmayr, A composite parameterization of unitary groups, density matrices and subspaces, J. Phys. A **43**, 385306 (2010).
[91] C. Spengler, M. Huber, and B. C. Hiesmayr, Composite parameterization and Haar measure for all unitary and special unitary groups, J. Math. Phys. (N.Y.) **53**, 013501 (2012).
[92] Wolfram Library archive, Composite parameterization and Haar measure for unitary groups, https://library.wolfram.com/infocenter/MathSource/7841/ (accessed 27.06.2020).
[93] R. Kitano, M. Koike, and Y. Okada, Detailed calculation of lepton flavor violating muon electron conversion rate for various nuclei, Phys. Rev. D **66**, 096002 (2002); **76**, 059902(E) (2007).